

The Effect of Norepinephrine Release on Odor Discrimination Learning in Adult Rats

by

© Faghihe Massaeli

A thesis submitted to the

School of Graduate Studies

in partial fulfilment of the requirements for the degree of

Master of Science in Medicine (Neuroscience)

Division of BioMedical Sciences

Faculty of Medicine

Memorial University of Newfoundland

May 2019

St. John's

Newfoundland

Abstract

The locus coeruleus is the main source of norepinephrine in the brain with extensive projections to many areas throughout the cortex including the olfactory bulb and piriform cortex. It has been shown that noradrenergic receptor blockade in either olfactory bulb or piriform cortex impairs similar odor discrimination. The goal of this thesis is to test whether enhancing locus coeruleus activity using optogenetic stimulation promotes odor discrimination learning.

Adult TH-CRE rats were bilaterally infused with adeno-associated virus containing light-excitabile channels targeting noradrenergic locus coeruleus neurons (AAV8-Ef1a-DIO-eChR2 (H134R)-EYFP). In vivo electrophysiology revealed neurons transfected with the viral vector were active when blue light (473 nm) was given at a frequency of 10Hz of 150mA laser current.

After confirming the excitability response of the neurons, we tested the effect of light on general locomotor activity. Subsequently, we sought to determine the role of locus coeruleus activation on odor discrimination learning. Food-deprived animals were trained to discriminate between two simple odors, one paired with a food reward. This training was followed by a highly similar odor discrimination in which animals were optogenetically stimulated with a phasic pattern of blue laser light. AAV-ChR2 infused rats discriminated the similar odors after 3 days of training, while non-infused control rats reached the learning criteria in 8 days. The enhanced LC activity induced by photostimulation during highly similar odor discrimination training promoted faster learning.

Acknowledgements

Grateful to God, completing my masters degree has been an incredibly rewarding experience. I was very fortunate to have tremendous support on my path to this accomplishment.

First and foremost, I would like to thank my supervisor Dr. Qi Yuan for her tremendous support, guidance, and dedication to helping me achieve this goal. She creates an open and supportive working environment where she is always willing to help. Her enthusiasm and incredible work ethic are both inspiring and motivating. I consider myself very fortunate to have had the opportunity to study in her laboratory. I have, and will always feel truly privileged to have been her graduate student.

I would like to thank my co-supervisor Dr. Christina Thorpe for her support and for her interest and help in this research project. I would also like to thank Dr. Carolyn Harley and Dr. Xihua Chen. Their enthusiasm for science and research is contagious and their brilliance is incredibly inspiring. I would also like to thank our research assistant Vanessa Strong for all her help, patience and kindness. She has been a huge help in teaching me the necessary laboratory techniques for this project.

Moreover, I would like to thank my family for their endless love and support and especially my husband, Sadra, for always being there when I need him. I am very blessed to have such amazing people in my life and I truly value the encouragement and faith that they have always shown in me.

Finally, I would like to thank the Natural Science and Engineering Research Council of Canada for their support in this project.

Contents

Abstract	ii
Acknowledgements	iii
List of Tables	vii
List of Figures	viii
List of Abbreviations	ix
1 Introduction	1
1.1 Overview	1
1.2 Norepinephrine Modulation in Behavioral Olfactory Processing	3
1.2.1 Cellular Organization of the Olfactory Bulb	7
1.2.2 Potential Cellular and Synaptic Mechanisms of NE in Learning	8
1.3 Locus Coeruleus	11
1.3.1 LC Anatomy and Function	11
1.3.1.1 Projections of the LC	14
1.3.1.2 LC Activity Patterns	15

1.4	Optogenetics	17
1.4.1	Optogenetic LC studies	18
2	Materials and Methods	21
2.1	AAV Infusion	22
2.1.1	Subjects	22
2.1.2	Viral Vector	22
2.1.3	Virus Infusion Surgery	23
2.1.4	Histology	25
2.1.5	Image Acquisition and Analysis	27
2.2	In Vivo Recording	27
2.2.1	Subjects	27
2.2.2	Electrophysiology Experiments	27
2.2.3	Data Analysis	29
2.2.4	Statistical Analysis	30
2.3	Behavioral Experiments	30
2.3.1	Optogenetic Cannula Implantation	30
2.3.2	Learning Promoting Effect	31
2.3.2.1	Subjects	32
2.3.2.2	Odorants	32
2.3.2.3	Habituation	32
2.3.2.4	Initial Procedure Learning	34
2.3.2.5	Difficult (Highly Similar) Odor Discrimination Training	34
2.3.2.6	Statistics	35

2.3.3	Mobility Effect	36
2.3.3.1	Subjects	36
2.3.3.2	Light Parameters Tests	36
2.3.3.3	Statistics	37
2.3.4	Histology	37
3	Results	39
3.1	In Vivo Electrophysiology Recording	39
3.2	Learning Promoting Effect	44
3.3	Mobility Effect	48
4	Discussion	53
4.1	Summary of Major Findings	53
4.2	In Vivo Electrophysiology Recordings	55
4.2.1	Light Patterns for LC Activation	55
4.2.2	Effect of In Vivo Photostimulation on LC Activation	57
4.3	Behavioral Effects of Optogenetic Stimulation	58
4.3.1	Light Patterns in Terms of Behavior - Mobility Effect	58
4.3.2	Effect of LC Photostimulation on Promoting Learning	60
4.4	Conclusions and Future Directions	61
5	Conclusions	64
	Bibliography	66

List of Tables

1.1	Timeline in research on the LC-NE system	11
2.1	Stereotaxic coordinates of LC for AAV-ChR2 infusion	24
3.1	Examples of tracking rats' bodies in the open field mobility test . . .	51

List of Figures

2.1	CRE recombinase mechanism.	23
3.1	In vivo optogenetic activation of LC with various light trains	41
3.2	Average AAV expression in LC cells.	43
3.3	Index of correct responses in simple odor discrimination training. . .	44
3.4	Latency to respond in simple odor discrimination training.	45
3.5	Index of correct responses in difficult odor discrimination training. . .	47
3.6	Latency to respond in difficult odor discrimination training.	48
3.7	Ratio of mobility time during photostimulation at different light frequencies to the baseline	49
3.8	Ratio of distance travelled during photostimulation at different light frequencies to the baseline	50
3.9	Npas4 immunoreactivity in LC neurons.	52

List of Abbreviations

AAV	adeno-associated virus
ANOVA	analysis of variance
aPC	anterior piriform cortex
ChR2	channelrhodopsin-2
DBH	dopamine β -hydroxylase
DIO	double-floxed inverted open reading frame
EF-1a	elongation factor 1a
EPL	external plexiform layer
ET	external tufted
EYFP	enhanced yellow fluorescent protein
GABA	γ -aminobutyric acid
Gal	galanin
GCL	granule cell layer
GFP	green fluorescent protein
GL	glomerular layer
Hz	hertz
IEG	immediate early gene
IPL	internal plexiform layer
ITI	inter trial interval
LC	locus coeruleus
LC-NE	locus coeruleus produced norepinephrine

m	meter
mA	milliampere
MCL	mitral cell layer
min	minute
mm	millimeter
ms	millisecond
mW	milliwatt
nAChRs	nicotinic acetylcholine receptors
NA	numerical aperture
NE	norepinephrine
nm	nanometer
NPAS4	neuronal PAS domain-containing protein 4
NPY	Neuropeptide Y
OB	olfactory bulb
ONL	olfactory nerve layer
OSNs	olfactory sensory neurons
PFA	paraformaldehyde
PG	periglomerular
s	second
SA	short axon
SD	standard deviation
SEM	Standard error of the mean
SEZ	subependymal zone

S/N	signal to noise ratio
TH	tyrosine hydroxylase
TH-Cre	tyrosine hydroxylase-Cre recombinase
vg/ml	viral genome per millilitres
μm	micrometer

Chapter 1

Introduction

1.1 Overview

Norepinephrine (NE) has been shown to modulate a variety of sensory systems, including olfactory processing at the behavioral and physiological levels. The olfactory bulb (OB) as the first central network in the olfactory pathway, is innervated by massive NE projection from the Locus Coeruleus (LC) (McLean, Shipley, Nickell, Aston-Jones, & Reyher, 1989; Sara, 2009). In rodents, approximately 40% of neurons in the LC project to the OB (Shipley, Halloran, & de la Torre, 1985).

In adult rats, NE is involved in modulating OB activity and responses. Brain slice recording data show that NE modulations result in an enhancement in signal to noise ratio (S/N) in the OB (Linster, Nai, & Ennis, 2011). *In vivo* evidence also confirms the effect of NE in increasing S/N at the OB output; and it is implied that the effect is via reducing the system's intrinsic noise level (Manella, Petersen, & Linster, 2017). This increased S/N at the OB output lowers the thresholds for odor detection and

discrimination (Escanilla, Arrellanos, Karnow, Ennis, & Linster, 2010; Manella et al., 2017).

It has also been shown in adult rodents that activating NE receptors influences different forms of plasticity in OB synapses (Doucette, Milder, & Restrepo, 2007; Mandairon et al., 2008; Linster et al., 2011; Manella, Alperin, & Linster, 2013; Shakhawat et al., 2015). Adrenergic blockade in OB slows down learning of two similar odor discrimination (Doucette et al., 2007; Mandairon et al., 2008; Shakhawat et al., 2015); while anterior piriform cortex (aPC) adrenergic blockade prevents similar odor discrimination learning (Shakhawat et al., 2015). These suggest a critical role for NE in olfactory processing and learning, particularly in a similar odor discrimination task. NE is implied to have a crucial role in the way an animal interacts in various behavioral states with its olfactory environment (Linster & Escanilla, 2018).

Would enhancing NE release facilitate odor discrimination learning? This thesis focuses on determining the role of enhancing LC activity on odor discrimination learning in adult rats. We first infused adult rats with the viral construct containing a light-activated ion channel. Three weeks or later following the infusions, we implanted animals with optogenetic cannulae to permit photostimulation of the LC. Age-matched control rats were also implanted with cannulae at the same time. After the recovery period, we performed *in vivo* recording to find the optimum light patterns for activating the LC. Based on the result obtained from *in vivo* recordings, another cohort of rats was then trained in a difficult odor discrimination task with light pulses given to the LC after simple discrimination pre-training. We hypothesize that enhanced LC activity by optical stimulation during odor discrimination training will induce faster learning via NE modulation of plasticity.

1.2 Norepinephrine Modulation in Behavioral Olfactory Processing

NE has been shown to influence olfactory processing at the behavioral and physiological levels. The OB, as the first central network in the olfactory pathway, is innervated by dense NE projections from the LC (Shipley et al., 1985; McLean et al., 1989; Sara, 2009) as well as inputs from a variety of modulatory systems, that are shown to have profound effects on odor memory and olfactory processing (Fletcher & Chen, 2010).

It has been reported that NE release in the OB plays a critical role in early olfactory learning (Sullivan & Wilson, 1991; Wilson & Sullivan, 1994; Yuan, Harley, Bruce, Darby-King, & McLean, 2000; McLean & Harley, 2004). In 1989, Sullivan et al. showed that blocking LC NE input in the OB inhibits acquisition of new memory (Sullivan, Wilson, & Leon, 1989). Early odor preference learning is a form of classical conditioning that shapes short-term or long-term behavioral preferences (Yuan, Shakhawat, & Harley, 2014). Newborn rats can be conditioned to a novel odor by stimulation that mimics the stimulation they experienced in maternal care paired with a novel odor (Yuan et al., 2014).

Odor preference learning can be acquired by pairing a novel odor with stimulation of LC (Sullivan, Stackenwalt, Nasr, Lemon, & Wilson, 2000) or when a novel odor is associated with α - or β -adrenoceptor activation (Morrison, Fontaine, Harley, & Yuan, 2013; Shakhawat, Harley, & Yuan, 2012; Harley, Darby-King, McCann, & McLean, 2006). It has been shown that the nature of early odor preference learning is associative, e.g., a novel odor being associated with a tactile stimulation induces the learning in pups (Sullivan et al., 1989). In rat pups, studies have shown that

pharmacological blocking of either α - or β -adrenoceptor in the OB or the aPC impairs early odor preference learning (Shakhawat et al., 2012; Morrison et al., 2013).

However, the role of NE in neonatal olfactory processes differs from adult odor learning (Linster & Escanilla, 2018). During the first week of life, preference learning in pups can even be acquired by associating a novel odor with a tail pinch (Sullivan, Hofer, & Brake, 1986) or mild foot shock (Camp & Rudy, 1988; Moriceau, Wilson, Levine, & Sullivan, 2006). However, after the first postnatal week (approximately after the first 10 days), training pups with associative stimulation will not induce odor preference learning (Yuan et al., 2014; Moriceau et al., 2006; Sullivan, Landers, Yeaman, & Wilson, 2000; Camp & Rudy, 1988).

In adult rats, NE is believed to be involved in modulating OB activity and responses. NE can modulate different aspects of olfactory processing: detection, encoding, retrieval, specificity and duration of an encoded odor memory (Linster & Escanilla, 2018). It has also been shown that in adult rodents, activating NE receptors influences different forms of plasticity in OB synapses (Doucette et al., 2007; Mandairon et al., 2008; Linster et al., 2011; Manella et al., 2013; Shakhawat et al., 2015).

The first step in olfactory processing is odor detection. NE can potentially modulate odor detection via increasing excitability of principal cells and decreasing baseline spontaneous activity (Linster et al., 2011; Nai, Dong, Linster, & Ennis, 2010). Brain slice experimental data show that NE modulation results in enhancement in S/N in the OB (Linster et al., 2011). *In vivo* evidence also confirms the effect of NE in increasing S/N at the OB output; and it is implied that the effect is via reducing the system's intrinsic noise level (Manella et al., 2017). This increased S/N at the OB

output causes lower thresholds in odor detection and discrimination (Escanilla et al., 2010; Manella et al., 2017).

However, behavioral studies on the effects of NE on odor perception have been controversial. In 1988, Doty et al. presented an experiment in rats testing thresholds of odor detection with chemical ablation of NE fibers in the OB. Their result showed no effect from this depletion on odor detection thresholds (Doty, Ferguson-Segall, Lucki, & Kreider, 1988).

On the other hand, other studies showed that rats infused directly with additional NE into their OB detected and discriminated odorants at lower thresholds of concentrations (Escanilla et al., 2010). These studies used a non-associative and spontaneous paradigm, which means there is no outside motivation for detecting odorants. In motivational reward learning, it has been shown that blockade of bulbar NE receptors slows, but does not prevent, odor discrimination learning (Shakhawat et al., 2015; Escanilla, Alperin, Youssef, Ennis, & Linster, 2012); however, aPC adrenoceptor blockade prevents similar odor discrimination learning and learning-induced changes in OB odor representations (Shakhawat et al., 2015).

A habituation task, using paradigms with multiple successive trials presenting repeated odorants, can be translated to an odor memory encoding process; and the speed of encoding can be assessed by observing investigation time over the trials (Linster & Escanilla, 2018). It has been shown OB α - and β - adrenoceptor blockade in rats had no effect on odor encoding in a task of habituation (Mandairon et al., 2008). In contrast, Guerin et al. showed mice with a chemical depletion of cortical noradrenergic fibers failed to habituate in the same paradigm; i.e., depletion of LC neurons led to a critical deficit in acquisition, in mice (Guerin, Peace, Didier, Lin-

ster, & Cleland, 2008). Either species or methodological differences may explain the contrasting effects in these studies.

The speed of acquisition in reward associative behavioral tasks can also be considered as reflecting the odor encoding process (Linster & Escanilla, 2018), experiments in several paradigms in mice and rats showed blocking OB α - and β - adrenoceptor slows down learning of two odor discrimination, i.e., impairs the encoding process (Doucette et al., 2007; Mandaïron et al., 2008; Shakhawat et al., 2015) in similar odor discrimination. Overall these data confirm the substantial role of NE in the odor encoding process.

Experiments using the olfactory recognition paradigm have shown that the noradrenergic system influences odor memory duration. Veyrac et al. investigated the effects of LC NE pharmacological modulations on olfactory recognition in mice. They exposed mice to a nonrewarded olfactory stimulation associated with an odor and performed odor discrimination recall tests after 15min, 30min and 60min. They showed in an odor discrimination recall test, NE depletion in the brain decreases memory of an encoded odor to 15 minutes, while NE enhancement increases memory duration to 30 minutes (Veyrac, Nguyen, Marien, Didier, & Jourdan, 2007). On the other hand, Manella et al. showed that in rats, NE infusion in the OB modulates odor recognition memory; decreasing memory duration in low and high dosages of infusions, and having no effect at medium dosage (Manella et al., 2013).

The controversial results of different experiments are likely due to the varied dosage of NE with different manipulations of the LC. Computational studies reveal that the effects of NE are non-linear and non-monotonic, which means the total dosage of NE determines the modulatory effects (Linster et al., 2011). On the other

hand, global manipulations such as electrical stimulation and global drug injection or chemical depletion of NE neurons have substantially different effects from local manipulations such as local NE or antagonist infusion (Linster & Escanilla, 2018). Thus the above data from different experiments are difficult to compare directly due to the differing nature of the procedures.

1.2.1 Cellular Organization of the Olfactory Bulb

The OB provides the first synaptic relay for sensory information in the olfactory pathway. It has a highly organized six-layered structure of distinct groups of neurons (Mori, 1987). From the most superficial moving inward, the layers are the olfactory nerve layer (ONL), glomerular layer (GL), external plexiform layer (EPL), mitral cell layer (MCL), internal plexiform layer (IPL), granule cell layer (GCL), and the subependymal zone (SEZ).

The axons of the olfactory sensory neurons (OSNs) are the most superficial layer of the OB and they collectively form the olfactory nerve layer which is the input area of the OB. The glomerular layer (with individual glomeruli) is comprised of processes of second-order projection neurons, mitral/tufted cells. The olfactory nerve terminals synapse within glomeruli, creating the first site of synaptic integration in the OB. The olfactory sensory neurons send and receive information via these synapses in the glomerular layer (Pinching & Powell, 1971).

There are three main types of neurons within the glomerular layer including periglomerular (PG) cells, external tufted (ET) cells and short axon (SA) cells. Together, these cells form a complex glomerular inhibitory network. The glomeruli are

surrounded by interneuron cell bodies and fiber-like structures that are composed of the axons from the olfactory sensory nerves as well as dendrites of the mitral cells (Belluscio, Lodovichi, Feinstein, Mombaerts, & Katz, 2002).

Inhibitory periglomerular cells inhibit mitral cells through feedforward inhibition. These PG cells are activated by olfactory nerve or sensory neuron activation, and feedforward to inhibit mitral cells.

The mitral cells have the biggest cell bodies and nuclei in the OB. Axons of mitral cell serve as the main output of the OB, receiving information from the olfactory sensory neurons (Yuan, 2009; McLean & Harley, 2004). Apical dendrites of the mitral cells synapse within the glomerulus, and lateral dendrites of the mitral cells make extensive synapses with the granule cells (Price & Powell, 1970).

Granule cells are also inhibitory interneurons which exert inhibition on mitral cells via lateral inhibition (i.e., activated granule cells inhibit other mitral cells through their synaptic connections), or feedback inhibition (i.e., granule cells, are activated by the mitral cells, and release GABA to inhibit the same mitral cells).

The glomerular layer, mitral cell layer, and granule cell layer are divided by layers of axons and dendrites known as the external plexiform layer and internal plexiform layer, respectively.

1.2.2 Potential Cellular and Synaptic Mechanisms of NE in Learning

NE receptors traditionally are in two categories of G-protein coupled receptors known as α and β receptors located both pre- and post-synaptically on neurons (Rogawski

& Aghajanian, 1982). The OB receives a massive noradrenergic input from LC, and adrenoceptors are found on different cell types of the OB (Schwarz & Luo, 2015). LC NE projections target primarily the internal plexiform, the granule cell, and the external plexiform layers (McLean et al., 1989). However, adrenoceptors are distributed in other layers as well.

α -receptors have two subtypes of $\alpha1$ and $\alpha2$ having excitatory and inhibitory effects, respectively (Aston-Jones & Cohen, 2005). β -receptors include three subtypes of $\beta1$, $\beta2$, and $\beta3$; the first two are located on the granule cell, internal plexiform layer and glomerular layers (Yuan, Harley, & McLean, 2003). $\beta1$ -receptors are highly expressed on mitral cells and periglomerular cells, and much lower on granule cells (Yuan et al., 2003). The external plexiform layer only expresses $\beta2$ -receptors (Woo & Leon, 1995).

NE release acts on $\alpha1$ -adrenoceptors on mitral cells and $\alpha1$ - and $\alpha2$ -adrenoceptors on granule cells (Linster & Devore, 2012). Activation of $\alpha1$ -receptors on mitral cells makes mitral cells more sensitive to weak and near threshold stimuli (Jiang, Griff, Ennis, Zimmer, & Shipley, 1996; Ciombor, Ennis, & Shipley, 1999). By activation of $\alpha1$ -adrenoceptors on granule cells, the inhibitory effects of granule cells on mitral cells increase thus, increasing S/N through lateral inhibition. In contrast, $\alpha2$ receptors on granule cells inhibits granule cells which decrease the inhibitory effects of granule cells on mitral cells (Aston-Jones & Cohen, 2005).

At low NE concentrations, $\alpha2$ receptors on granule cells are activated, which decreases the inhibition of mitral cells (Nai et al., 2010). Thus, when NE is low, mitral cells are excited, also $\alpha1$ receptors on mitral cells make the cells more responsive to peri-threshold stimuli (Linster & Devore, 2012; Jiang et al., 1996; Ciombor et al.,

1999). Activation of $\alpha 1$ -adrenoceptors on mitral cells, enhances GABAergic inhibition of mitral cells (Nai, Dong, Hayar, Linster, & Ennis, 2009), sharpens their response to stimuli, i.e., increasing "signal" in S/N. Hence, at low NE concentrations, mitral cells are more sensitive to the stimuli.

At medium NE concentrations, granule cells are affected, mitral cells are still sensitive and respond more specifically to the stimuli.

At higher NE concentrations, in granule cells, the inhibitory effect of $\alpha 1$ receptors dominates over the excitatory effect of $\alpha 2$ receptors. Thus, because of the inhibitory effect of granule cells, mitral cells are inhibited, they become less sensitive (Escanilla et al., 2010; Nai et al., 2010). By increasing NE release, $\alpha 1$ receptors on granule cells are activated, they enhance the inhibitory effect of granule cells, consequently, inhibit mitral cells (Linster & Devore, 2012).

In a nutshell, activation of $\alpha 1$ -adrenoceptors on mitral cells enhances their sensitivity to the olfactory sensory inputs, and enables these cells to respond to weak stimuli, which is in fact impairing discrimination. At the same time, activation of granule cells accompany this process and preserve discrimination at higher NE concentrations (Linster & Devore, 2012). In fact, activation of granule cells and release of GABAergic input to mitral cells, limits spontaneous activity, consequently decreases noise. This conclusion is verified in behavioral experiments showing that by infusing NE into the OB, both perceptual and discrimination threshold was decreased (Escanilla et al., 2010).

The output result is that with increasing NE concentrations, cells become more affected and more NE enhances the network excitability. On the other hand, $\alpha 1$ -adrenoceptors in mitral cells, enhance the response to stimuli, i.e., increasing signal

in S/N; meanwhile activation of granule cells and release of GABAergic input to mitral cells, limits spontaneous activity, consequently decreases noise (Escanilla et al., 2010). Thereby, the net effect is increased S/N as well as enhancement of network excitability (Linster & Devore, 2012).

1.3 Locus Coeruleus

1.3.1 LC Anatomy and Function

The LC is a small nucleus located bilaterally in the pons of the brainstem. Despite its small size of around 1500 neurons in the rat, 15,000 in the human per hemisphere (Uematsu, Tan, & Johansen, 2015), it has more noradrenergic neurons than any other brain structure and provides the sole NE projections to many brain areas (Berridge & Waterhouse, 2003; Aston-Jones & Cohen, 2005; Samuels & Szabadi, 2008). The LC-NE system innervates the majority of forebrain structures and has broad connections to a wide variety of neuronal circuits (Berridge & Waterhouse, 2003), and cognitive tasks, including facilitating synaptic plasticity (Cooke & Bliss, 2006).

Table 1.1: Timeline in research on the LC-NE system

1812	The first anatomical description of the LC was presented. (Wenzel & Wenzel, 1812)
1949	Moruzzi and Magoun described the ascending reticular activating system and LC as a part of it and received a Nobel prize for their work. (Moruzzi & Magoun, 1949)

1964	The noradrenergic nature of the LC was identified. (Dahlstrom & Fuxe, 1964)
1969	The role of LC in the regulation of sleep was specified. (Roussel, Buguet, Bobillier, & Jouvet, 1967)
1972	A hypothesis about the important role of the NE in learning, LTP and memory processes was presented. (Kety, 1972)
1975	Modulatory effect of NE on S/N in the monkey auditory system was shown. (S. L. Foote, Freedman, & Oliver, 1975; Swanson & Hartman, 1975)
	The widespread efferent projections of the LC were shown (Swanson & Hartman, 1975)
1978	The afferent projections to the LC were found (Cedarbaum & Aghajanian, 1978)
	The role of the LC-NE system in reward and attention was identified (Mason & Iversen, 1978)
	The effect of the LC in morphine addiction was described (Aghajanian, 1978)
1981	The first paper on <i>in vivo</i> recordings of the LC activity in behaving rats, showing the role of LC in vigilance was published. (Aston-Jones & Bloom, 1981a)
1983	The first description of frequency-independent long-lasting potentiation by NE was made (Neuman & Harley, 1983)

1985 An early attempt to relate S/N effects of NE to cognitive function. The LC was shown to have an effect on memory retrieval (Sara, 1985a, 1985b)

Information in the table are given from the review study by Susan J. Sara, 2009.

While all LC cells are noradrenergic, they have other different components that make them capable of various functions (Schwarz & Luo, 2015). Various studies have examined the molecular diversity of neurons existing within this small nucleus which has shown they are much more diverse than their primary function as NE-producing neurons. There are at least two types of noradrenergic neurons within the LC; the large multipolar cells located more in the ventral LC and smaller fusiform cells more in the dorsal LC (Swanson, 1976; Grzanna & Molliver, 1980).

Different neuropeptides are expressed within the LC cells. The most important ones are galanin (Gal) and Neuropeptide Y (NPY) which are expressed in NE⁺ LC neurons (Schwarz & Luo, 2015). Galanin is found in up to 80% of noradrenergic LC (Holets, Hökfelt, Rökaeus, Terenius, & Goldstein, 1988). Lang et al. reviewed the modulatory effect of galanin in many behaviors such as nociception, sleep/wake states and feeding (Lang et al., 2015). Gal⁺ neurons are located throughout the LC and are more densely found in dorsal and central LC sub-areas (Holets et al., 1988). A smaller number of LC neurons (nearly 20%) co-expressing NE and Neuropeptide Y are more localized to the dorsal LC (Holets et al., 1988).

Various neurotransmitter and neuropeptide receptors are present in LC neurons including $\alpha 1$ and $\alpha 2$ adrenoceptor subtypes, nicotinic acetylcholine receptors (nAChRs),

GABA, orexin/hypocretin and opioid receptors (Schwarz & Luo, 2015). These receptors could make a significant difference in how subtypes of LC cells respond to an input signal.

1.3.1.1 Projections of the LC

The LC consists of a small number of NE neurons that project broadly throughout the brain and receive input from various brain areas. Despite its small size, LC neurons have substantial postsynaptic projections, which extend hundreds of micrometers beyond the compact nucleus with axonal projections distributing throughout the neuraxis, from the spinal cord to the neocortex (Shipley, Fu, Ennis, Liu, & Aston-Jones, 1996; Uematsu et al., 2015).

Loughlin et al. have presented the spatial organization of rat LC neurons projecting to particular brain regions. For instance, dorsal LC regions innervate the forebrain, while ventral portions participate in projections to the cerebellum and spinal cord. The anterior regions of LC send projections to the thalamus and hypothalamus, meanwhile dorsal and posterior regions of the LC project to hippocampus, forebrain and other regions of the cortex (Loughlin, Foote, & Bloom, 1986).

From the brainstem and midbrain, LC modulates neural processing with interconnections to visceral and sympathetic nervous system (Cedarbaum & Aghajanian, 1978). In addition, LC regulates highly processed emotional and cognitive information by its connection to forebrain structures (Berridge & Waterhouse, 2003; Uematsu et al., 2015). This nucleus is interconnected with neuromodulatory brain regions including the ventral tegmental area (dopamine) and dorsal raphe (serotonin) (Uematsu et al., 2015).

Moreover, it has been shown that a single LC neuron can project to different brain areas (Mason & Fibiger, 1979); individual LC neurons have the ability to send axons to functionally correlated, yet discrete portions of ascending sensory pathways (Simpson et al., 1997; Berridge & Waterhouse, 2003).

1.3.1.2 LC Activity Patterns

Noradrenergic systems are an essential part of sensory processing that support fore-brain activation in different types of behavior. Behaviors are classified into two general categories in rodents. The first "Type I" are voluntary and determined behaviors such as locomotor activities and isolated movements of the head (for instance as a sign of attention). These behaviors have been associated with hippocampal EEG activation, e.g., theta activity (Vanderwolf & Robinson, 1981) as well as the increase of LC discharge rate (Berridge & Waterhouse, 2003). Meanwhile, "Type II" behaviors are automatic-type including grooming, licking, chewing, etc. are not associated with hippocampal theta activity. In these behaviors, LC neurons display low discharge rates (Berridge & Waterhouse, 2003).

During the awake state, NE neurons of the LC-NE system naturally fire in distinguishable activity modes in response to various environmental challenges referred to as tonic and phasic. Tonic activity is described as a sustained lower frequency in regular firing patterns; it is often state-dependent, with the highest firing rates occurring during waking, and the lowest during slow-wave and REM sleep (Hobson, McCarley, & Wyzinski, 1975). Tonic activity can be divided further into two categories of low- and high-tonic. While the subject is involved in everyday behaviors including eating and grooming, LC cells fire in a slow, rhythmic pattern around $1 - 3Hz$, which is

consistent with an awake state (Carter et al., 2010, 2012). High tonic is $3 - 8Hz$ LC discharge which is active with stressful events and stimuli (Reyes, Drolet, & Van Bockstaele, 2008; Curtis, Leiser, Snyder, & Valentino, 2012). It has been shown in a recent study that stimulating LC high tonic activity using designer receptors (DREADDs) impaired task performance, increased response times and decreased task participation (Kane et al., 2017). Tonic firing rates as high as $15Hz$ have been reported for a limited duration, under high arousal conditions (Berridge & Waterhouse, 2003).

LC neurons can also fire phasically in response to sensory stimuli, such as touch, flash of light, auditory tones or stimuli that interrupt stereotypical behaviors. Phasic responses normally are shorter in latency and are a brief burst of firing, followed by a more prolonged period of suppression (S. Foote, Aston-Jones, & Bloom, 1980). Phasic bursts are typically $8 - 10Hz$ firing (McCall et al., 2015; Aston-Jones & Bloom, 1981b). In rodents, the burst firing mode has been shown to activate in classical conditioning when salient stimuli are presented and to terminate when the conditioning is established (Linster & Escanilla, 2018).

In the phasic mode, the LC has a burst of activity which is driven by the decision processes in response to a specific task. This burst of firing produces a broad release of NE, increasing the gain of cortical processing units and facilitating task-relevant behavior (Aston-Jones & Cohen, 2005). In other words, LC phasic response serves as a temporal attentional filter, the burst of firing is specific to the event, facilitating the corresponding processes, thereby increasing the performance of the current task relative to other distracting events (Aston-Jones & Cohen, 2005).

On the other hand, the tonic firing mode increases the baseline NE release, which increases responsivity of target neurons to a wider range of environmental events

(Aston-Jones & Cohen, 2005). By occurring in a stimulus-related manner, the LC phasic response and consequence burst release of NE promotes the event-related attention needed; but in a stressful situation, helps the animal to attend to a broad variety of surrounding events.

The distinct LC activity patterns optimize the trade-off between retaining reliable sources of reward while exploring new chances in a changing environment.

1.4 Optogenetics

In recent years, optogenetics research has been used in a wide range of animal models. Optogenetic experiments in rats are limited because of the lack of viral promoters which are capable of driving specific expression. By the development of transgenic rat lines expressing Cre recombinase, rat models became capable of optogenetics (Fenno, Yizhar, & Deisseroth, 2011). In these models, a Cre recombinase/LoxP system can modulate a specific gene expression, which is necessary for studying or utilizing a specific protein or peptide in a group of cells.

For cell type-specific targeting, a Cre-inducible viral vector containing the gene encoding the light-activated channel, under the control of a promoter is utilized. To ensure that the expression is specific to targeted cell types the viral construct will be designed with the opsin sequence in the opposite orientation. Upon delivery of this viral construct stereotactically into the targeted cells, Cre-expressing cells flip the opsin into the correct orientation and thereby activate the expression specific to the targeted cells (Tsai et al., 2009) (Figure 2.1).

In vivo optogenetic modulation in anesthetized animals, has been employed with

optrodes which are composed of an optical fiber coupled with tungsten electrodes (Fenno et al., 2011).

In optogenetic experiments performed on awake behaving animals, the conventional approach is to connect the light source to implanted cannulae via optical fibers. However, this physical cord connection has disadvantages such as restricting natural movement of the animal as well as distracting the animal with the cord hooked up to their head. To eliminate this issue, a wireless optogenetic system has been developed and utilized in a mouse study by Rossi et al. (2015). They optically stimulated the striatum and observed robust twitching and circling behaviors which were frequency dependent (Rossi et al., 2015).

1.4.1 Optogenetic LC studies

Several studies have manipulated LC optically in transgenic tyrosine hydroxylase-Cre recombinase (TH-Cre) mice. In these studies, it has been shown that different behaviors are a consequence of distinct LC firing patterns. In fact, these studies nicely demonstrate the importance of distinct LC firing patterns in generating various and sometimes contrasting behaviors.

In one study, Carter et al. (2010) optically controlled the firing rate of LC-NE neurons in awake-behaving mice. They showed that optogenetic stimulation of the LC neurons in awake-behaving mice modulates their locomotor activity which was dependent on the light pattern as well as the length of the stimulation period to the LC. They showed that $1h$ tonic stimulation with a $3Hz, 10ms$ light pulses increases general mobility while phasic stimulation with $10Hz, 10ms$ light pulses in

burst duration of 500ms every 20s decreases the mice mobility over the hour of stimulation (Carter et al., 2010).

Carter et al. (2010) also showed LC activation regulates the duration of wakefulness and also promotes immediate sleep-to-wake transitions, reducing the amount of time the subjects spent sleeping. However, they observed that inhibiting LC did not increase the sleeping period (Carter et al., 2010).

Another researcher (McCall et al., 2015) also used optogenetics to manipulate LC firing rate in stress-induced behaviors in mice. In this way, the authors confirmed that high-frequency tonic, activation of the LC could evoke anxiety and aversion behaviors. This anxiety-like behavior was not observed in phasic stimulation. Interestingly, they found that inhibiting the LC chemogenetically during stressful stimuli prevented the consequent anxiety.

Tonic versus phasic LC photostimulation generates distinct behaviors:

- Both induce sleep-wake transition (Carter et al., 2010)
- Both increase duration of wake episodes (Carter et al., 2010)
- Tonic increases locomotion (Carter et al., 2010)
- Tonic generates anxiety-like behavior (McCall et al., 2015)
- Phasic decreases locomotion (Carter et al., 2010)

Another study in rats by Hickey and colleagues investigated the known role of LC in the descending pain control circuit. The rats in this experiment were optically stimulated in a population of LC neurons. Depending on the specific area of LC neurons that were stimulated the nature of the responses were different. Post-hoc

histological analysis showed that rats with antinociceptive responses had more ChR2⁺ cells located in the ventral LC, while pronociceptive rats had more ChR2⁺ neurons in the dorsal LC (Hickey et al., 2014). Therefore, they demonstrated that biased populations of LC-NE neurons result in distinct behaviors.

Chapter 2

Materials and Methods

The primary purpose of the following experiments was to understand the effect of LC phasic activation on learning in adult rats. With the optogenetic manipulation of LC, we investigated the effect of various patterns of photostimulation on LC activity. We also aimed to gain insight into how different firing modes of the LC cells affect animal's behavior in different aspects such as learning and locomotor activity. Adult rats were first infused with the viral construct containing the light-activated channel; following that we performed *in vivo* recording to identify the effective light patterns for activating LC. Another cohort of rats was then trained an odor discrimination task with a selected light pattern given to the LC. We hypothesize that LC activation by phasic optical light pattern during odor discrimination training leads to learning facilitation. The details of outlined experiments are described in this chapter.

2.1 AAV Infusion

2.1.1 Subjects

TH-Cre Sprague Dawley rats were used in this study. Animals were bred from homozygous TH-Cre males, obtained from Sage Laboratories (Boyertown, Pennsylvania, USA) and Sprague Dawley females, obtained from Charles River (Saint-Constant, Quebec, Canada). Total number of animals who included in the study was 37 and some animals were used in different behavioral experiments to minimize animal use. Animals were housed in individual cages on a standard light-dark cycle, receiving food and water *ad libitum*. All procedures were approved by the Institutional Animal Care Committee at Memorial University of Newfoundland and followed the guidelines set by the Canadian Council on Animal Care.

2.1.2 Viral Vector

For cell type-specific targeting, we used a Cre-inducible adeno-associated virus (AAV) vector containing the gene encoding the light-activated channel, under the control of the elongation factor 1a (EF-1a) promoter. The viral vector was AAV8-Ef1a-DIO-eChR2 (H134R)-EYFP with a titer of 1.20×10^{14} , in a working solution of $5 \times 10^{12} \text{ vg/ml}$, provided by Dr. Deisseroth's lab at Stanford University (Deisseroth, K., Stanford University, Stanford, CA, USA).

The genes were comprised of a rhodopsin-driven excitatory channel, channelrhodopsin-2 (ChR2) in-frame fused to enhanced yellow fluorescent protein (EYFP). EYFP is coupled with the channel to enable the visualization of ChR2-expressing cells. The

excitatory channel is channelrhodopsin-2 with the H134R mutation that has a slight reduction in desensitization and an increase in sensitivity in response to light and slower channel closing in comparison to ChR2 (Lin, 2011).

To ensure that the expression is specific to targeted cell types, the viral construct is designed with a double-floxed inverted open reading frame (DIO) such that the ChR2-EYFP sequence is in the opposite orientation. We deliver this viral construct stereotactically into the LC of tyrosine hydroxylase (TH) Cre transgenic rats. Upon transduction, Cre-expressing TH cells flip the ChR2-EYFP DIO into the correct orientation and thereby activate the expression specific to TH positive cells (Tsai et al., 2009) (Figure 2.1). The efficacy and specificity of targeting was validated *in vivo*.

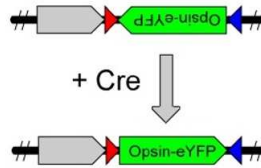


Figure 2.1: CRE recombinase mechanism.

2.1.3 Virus Infusion Surgery

Animals were anesthetized with isoflurane (15%) and were given subcutaneous injections of Meloxicam (Metacam, Boehringer Ingelheim Canada Ltd., Burlington, ON, Canada) analgesia with a dosage of 0.1mg/kg body weight, diluted in 0.9% sodium chloride. The surgical area on the rat's head was shaved, and tear gel was applied to prevent the rat's eyes from drying during the surgery. Rats then were fixed in a stereotaxic apparatus in the skull flat position, on a heating pad to maintain internal body temperature at approximately 37°C . The surgical area was sterilized with

chlorhexidine scrub, then swabbed with 70% isopropyl alcohol and betadine tincture.

A single incision was made along the midline and the skin was retracted to expose the skull. Stereotaxic coordinates were taken from lambda and bregma to adjust the skull flat position. Holes were drilled over the locations of LC in coordinates of $11.8 - 12.3mm$ posterior and $\pm 1.3mm$ lateral to bregma (Table 2.1).

Holes then were cleared of debris. An internal cannula was lowered at an angle of 20° anterior to the vertical, to a depth of $5.5mm$ below the surface ($-6.5mm$ from the skull) and a $0.5\mu l$ aliquot of AAV8-Ef1a-DIO-eChR2 (H134R)-EYFP virus was infused in each hemisphere, for a total of $1.0\mu l$ bilaterally. All infusions were completed using a Hamilton $1.0\mu l$ syringe over the span of 5 minutes ($0.1\mu l/min$), using a NE-4000 programmable 2 channel syringe pump (New Era Pump Systems Inc., Trumbull, CT, USA).

Table 2.1: Stereotaxic coordinates of LC for AAV-ChR2 infusion

Stereotaxic Coordinates			Rat's Weight		Population	
A/P	M/L	D/V	Male	Female	Male	Female
-11.8	± 1.3	-5.5	252.00 ± 4.94	211.17 ± 33.01	5	6
-12.0	± 1.3	-5.5	554.00 ± 35.69	335.00 ± 20.00	4	2
-12.3	± 1.3	-5.5	591.33 ± 55.84	657.00 ± 0.00	12	1
Stereotaxic coordinates are in millimetre, Rat's weight is in gram (mean \pm SD)						

Before removing the cannula, an additional 5-10 minutes given to ensure the infusion was complete. The incision was then closed with five to six sutures. Rats were then put in a clean cage and placed on a heating pad until they awoke.

Following the infusion surgeries, animals were caged in single cages, given food and water *ad libitum* and kept on a standard dark-light schedule. Rats had an recov-

ery period of at least three-weeks post-surgery, to permit adequate levels of channel expression.

2.1.4 Histology

Following all experiments, rats were transcardially perfused with ice-cold 0.9% saline solution, and ice-cold fixative 4% paraformaldehyde (PFA) in 0.1M phosphate buffer, pH = 7.4, solution. Brains were removed and stored at 4 °C in 4% PFA for 24 hours and then immersed in 20% sucrose (made in 0.1M phosphate buffer) solution for another 24 hours at 4 °C and stored under same conditions until sectioning.

For sectioning, brains were removed from the storage sucrose solution and quick-frozen on dry ice. The LC was cut into 30 μ m coronal sections in a Microm HM550 Cryostat at -20°C . Sections were then stored in PVP cryoprotectant (1% polyvinylpyrrolidone, 30% sucrose, 30% ethylene glycol in 0.1M PBS) storage solution until used for immunohistochemistry.

An alternating set of sections was mounted directly onto chrome-gelatin coated slides, air-dried at room temperature, and stained using a Nissl staining protocol for perfused tissue to determine LC sections for immunohistochemistry.

The Nissl staining procedure required first dehydrating the tissue by immersing it in 70%, 95%, 100% ethanol (2min each), and xylene (1min) followed by a quick wash in distilled water ($\times 3$). Then rehydrating the tissue with ethanol (100%, 95%, and 70%) followed by a three times quick wash in distilled water. Sections then were immersed in 1% Cresyl violet for 2-3 minutes followed by washes in distilled water. This was subsequently followed by one dip in 1% acetic acid and immediately

in distilled water ($\times 3$). Dehydration step proceeded again, and slides remained in xylene until coverslipped with Permount mounting medium.

After confirming the placement by Nissl stained sections, for visualizing LC by the DBH immunohistochemical marker, adjacent free-floating LC sections were used. Sections were washed in Tris buffer (0.1M, pH = 7.6) at five minute intervals ($\times 3$) to remove remaining PVP solution. Sections then were washed in 1% hydrogen peroxide (30min) followed by five minute washes in Tris buffer($\times 3$), Tris A (0.1% Triton X in Tris buffer), and Tris B (0.1% Triton X and 0.005% BSA in Tris buffer). Sections were then incubated in 10% donkey serum (Sigma-Aldrich Inc. St. Louis, MO, USA) in Tris B, for one hour as a blocking buffer to reduce non-specific immuno-staining; followed by two 10 minute washes in Tris A and Tris B. Sections were then incubated in anti DBH primary antibody (Millipore, Etobicoke, Ontario, Canada) at a 1:10000 dilution in Tris B for two days in a 4°C humidified chamber.

On the second day of the immunohistochemistry procedure, sections were first washed in Tris A and Tris B, each for 10min and were next incubated in donkey anti mouse secondary antibody, Alexa Flour 555 (Thermo Fisher Scientific Inc., Carlsbad, CA, USA) diluted 1:400 in TrisB for 45min followed by three 5min washes in Tris buffer and mounted on slides and coverslipped via Vectashield hard set mounting medium with DAPI (Vector Laboratories, Burlingame, CA, USA). In all steps, sections were transferred to new wells by brush. Slides were stored at 4°C until dried and ready for imaging.

2.1.5 Image Acquisition and Analysis

Processed sections were next imaged with a BX-2 brightfield microscope with a DP-72 digital camera, applying the appropriate filters when needed at $10\times$ – $40\times$ magnification. ImageJ software was used for counting cells manually. Counts were obtained for the number of green fluorescent protein (GFP) and DBH cells.

2.2 In Vivo Recording

2.2.1 Subjects

Subjects that were included in the study were three TH-Cre male rats, 23 – 30 weeks old, 600 – 675g at the time of the experiments. These are the animals with correct placement of the virus and optrode during the recording. Animals were housed under a standard light/dark cycle in single cages with *ad libitum* food and water. All procedures were consistent with Canadian Council of Animal Care guidelines and were approved by the Memorial University Institutional Animal Care Committee.

2.2.2 Electrophysiology Experiments

In vivo electrophysiology experimentation on rats was performed at least four weeks after virus infusion surgeries. The optrode was assembled prior to each experiment. The optrode consists of a $400\mu m$ glass optical fiber (Thorlabs Inc., Newton, NJ, USA) bundled securely with a $200/280\mu m$ tungsten electrode (FHC, Bowdoin, ME, USA).

Rats were anesthetized in their home cage with 15% urethane $10ml/kg$ of their body weight. The surgical area on the head was shaved. Rats then were fixed in a

stereotaxic apparatus, on a heating pad to maintain internal body temperature at approximately 37°C .

A single incision was made along the midline, and the skin was retracted to expose the skull. Stereotaxic coordinates were taken from lambda and bregma to achieve skull flat. A hole was drilled over the location of LC in the left hemisphere at the coordinates of 12.3mm posterior and $1.2 - 1.3\text{mm}$ lateral to bregma and was cleared of debris. An additional hole was drilled in the contralateral hemisphere, and a screw was placed. The skull screw, as well as stereotaxic apparatus, were grounded.

The hand-constructed optrode was lowered at the angle of 20° anterior to the vertical, to a depth of $5.3 - 5.5\text{mm}$ below the surface of the brain until putative LC cells could be identified utilizing both audio-monitor and oscilloscope. The criteria were a slow spontaneous firing frequency and a burst response to tail or toe pinch.

The glass optical fiber was connected to a Laser Diode Fiber Light Source: 1-channel model (Doric Lenses, Quebec City, Quebec, Canada). The central wavelength of light was 473nm (blue light) with the power of 90mW when coupled into a $400\mu\text{m}$ core, 0.48 NA optical fiber. Each laser light source was connected to a Mono Fiber-optic Patch Cord (Glass, 0.48 NA, $400/430\mu\text{m}$) via an FC connector. Fiber-optic Patch Cords were connected to the glass optical fiber via zirconia mating sleeves (1.25mm ferrule diameter). The laser light source was connected to a computer controlled with Doric software to control light pattern.

Several parameters were applied to determine an effective light pattern of stimulating LC. Laser light sequences with frequencies ranging from $1 - 30\text{Hz}$ and pulse widths of $10 - 50\text{ms}$ with currents of $75 - 150\text{mA}$ were applied. Each sequence lasted for 10s and was separated by at least two minute intervals allowing for a pre-light

time of resting cellular activity, as well as a post-light period to allow the cell to return to its baseline. Cells firing in the proximity of electrode tip were recorded by DataWave allowing for later analysis.

Rats were then perfused with ice-cold 0.9% saline solution, and ice-cold fixative 4% PFA (paraformaldehyde in 0.1 M phosphate buffer) solution. Brains were removed and stored at 4 °C in 4% PFA for 24 hours and then immersed in 20% sucrose (made in 0.1M phosphate buffer) solution for another 24 hours at 4 °C, then stored under the same conditions until sectioning and immunohistochemistry.

2.2.3 Data Analysis

The thresholds of analysis were set to only count cells at least $1.5\times$ bigger in amplitude than the background; this lower limit is used to ensure adequate signal to noise discrimination of units. Relevant features of cell waveforms were extracted using the autosort protocol in DataWave. Similar cellular waveforms were then separated and assigned to one cluster. Each cluster represents a cell. Of those clusters, the ones that displayed LC spike characteristics were included in statistical analyses. Next, frequency histograms were completed within DataWave for each light trial and each unique waveform respectively; these histograms provide the frequency of cells firing per second, with one minute baselines collected before and after the light protocol. Frequency histograms were then completed in OriginPro to compare the firing rate of LC cells before, during and after each light protocol to determine changes in activity.

2.2.4 Statistical Analysis

One-way analysis of variance (ANOVA) was performed to analyze differences in neuronal firing rate before, during and after the light pulses for each light pattern. Additional testing, by way of Tukey post hoc tests, were run to examine any specific differences between the neuronal firing patterns before and during, before and after, and during and after light pulses.

2.3 Behavioral Experiments

2.3.1 Optogenetic Cannula Implantation

26 TH-Cre rats were divided into AAV-ChR2 infused and control (no infusion) cohorts, 13 rats per cohort. At least three weeks post virus infusions in the AAV-ChR2 group, animals were implanted with the optogenetic two-ferrule cannula to permit photostimulation of the LC. Age-matched control rats were also implanted with cannula at the same time. Control group did not undergo virus infusion surgery and had only one surgery of implanting cannula.

Animals underwent the same surgical procedure steps as described in section 2.1.3. Holes were drilled over the locations of LC in coordinates of $12.3mm$ posterior and $\pm 1.25mm$ lateral to bregma. Holes then were cleared of debris. In addition to LC holes, four screw holes were drilled posterior and lateral to bregma. Dental cement sticks to the surface through the metal screws on the skull.

An optogenetic two-ferrule cannula was lowered at the angle of 20° anterior to the vertical, to a depth of $5.5mm$ below the surface. The two-ferrule Cannula has two

implantable flat tip fibers with the length of $1mm$, with a core diameter of $400\mu m$ and an outer diameter of $430\mu m$ each within its own ferrule, at a distance of $2.5mm$.

To secure the location of two-ferrule cannula, we then applied dental cement to the surface of the skull surrounding the cannula in three thin layers. The dental cement was a mixture of Ortho-Jet Liquid and Jet Denture Repair Powder (Lang Dental Manufacturing Co., Inc, IL, USA). Antibiotic was mixed with the powder to prevent infections. When the dental cement was hardened, the front part of the incision was closed using two to three sutures. Rats were then put in a clean cage and placed on a heating pad until they awoke.

Following the cannula implantation surgeries, animals were caged in single cages, given food and water *ad libitum* and kept on a standard light-dark cycle. Rats then had at least one week for recovery before starting the behavioral experiments.

2.3.2 Learning Promoting Effect

TH-Cre rats were divided into AAV-ChR2 infused and control (no infusion) cohorts. A week following the cannula implantation surgery, rats underwent behavioral experiments, which consisted of three stages: habituation, initial simple odor discrimination procedure learning, and difficult odor discrimination. This final set of training involved a series of two highly similar odor mixture pairs, one was associated with an appetitive food reward, while LC was photostimulated. This procedure assessed the effect of LC activation on difficult odor discrimination learning. Details of the procedure are described in the following sections. Optogenetic devices and supplies were ordered from Doric (Doric Lenses Inc, Quebec, Canada).

2.3.2.1 Subjects

Subjects were twelve TH-Cre male rats, grouped as seven AAV-ChR2 injected and five age-matched control rats, approximately seven months old at the time of the experiment. Animals were housed under a standard light/dark cycle in single cages with *ad libitum* food and water, except during behavioral training. They were under food deprivation five days before training began -one day before habituation stage began- with the total amount of roughly 12g food per day. All procedures were consistent with Canadian Council of Animal Care guidelines and were approved by the Memorial University Institutional Animal Care Committee.

2.3.2.2 Odorants

The simple odor pair was 6.632% of terpinene versus 2.673% of 1-octanol in mineral oil solution (Devore, Lee, & Linster, 2013) and the similar odor pair was 1-heptanol 1-octanol 40% : 60% (%*vol/vol* = 0.001) versus 1-heptanol 1-octanol 50% : 50% (%*vol/vol* = 0.001) in mineral oil solution (Shakhawat et al., 2015).

2.3.2.3 Habituation

Rats were first exposed to the experimental box and the food used for the procedure. The experimental chamber was a $100 \times 100 \times 60\text{cm}$ opaque Plexi box. Chocolate cereal was the appetitive food reward used for training.

Two sponges were placed in the chamber and used to present the odorants. Food reward was put in the 2cm deep hole in the center of one sponge. To balance the chocolate smell in the background in both sponges, a chocolate cereal was hidden in

the other sponge as well, however it was not retrievable. Animals were habituated to the behavioral chamber for four days until they became accustomed to it. Both sponges were unscented during the habituation period.

The first day of habituation was a single trial session and lasted until the animal retrieved the reward in the hole of the sponge, which was at least $15min$ with a ceiling of $30min$. If the animal retrieved the reward in less than $15min$, he was allowed to be in the box for a couple of additional minutes, so that all animals were at the same level of exposure to the experimental box and environment.

On the second day of habituation, rats were also exposed to the barrier which is an opaque Plexi L-shape wall that was used to keep them in a corner of the chamber in the inter trial intervals (ITIs). This corner was always a same corner, which was considered the starting point throughout the experiment. The second day was a three to five trials session, and the location of the sponge was randomized across the trials. ITIs were $30s$.

The third and fourth days of habituation were a ten trials session, with the location of the unscented sponges randomized between trials. Each trial lasted until animals retrieved the reward, otherwise there was a ceiling of $3min$. Rats were moved back to the starting corner using the barrier during ITIs. ITIs were not longer than $10s$.

Laser light sources were connected to the cannulae on the animal's head using a $1m$ patch cord. Light sources were off, and the objective was for the animals to be accustomed to the cord hooked up to their head, before starting training.

2.3.2.4 Initial Procedure Learning

The $60\mu l$ of odorant was applied to the sides of $S+$ and $S-$ sponges. Terpinene odor ($S+$) was introduced with the food reward (2-3 piece of chocolate cereal in the center hole of the sponge), while there was no reward associated to 1-octanol odor ($S-$). Training was performed as daily sessions during the light cycle of the rats and consisted of a series of ten trials. Rats were allowed to explore the box and sniff the sponges until they did a nose poke to the center hole of one of the sponges. The first nose poke was considered as the rat's response, and once the rat had the first response, correct or wrong, the trial was stopped. The ceiling time for each trial was three minutes. Then the rat was moved back to the starting corner using the barrier, the barrier was put in the chamber, the location of both sponges was changed, the barrier was lifted, and the next trial was started.

Discrimination learning was defined as $> 80\%$ correct responses in two consecutive sessions. Laser light sources were off; however, the patch cord was connected to the rats' head during all the training time. Training was video recorded and rats were tracked with ANY-maze behavior tracking software (Stoelting Co., Wood Dale, IL, USA). All rats learned to discriminate between the two odors within seven days.

2.3.2.5 Difficult (Highly Similar) Odor Discrimination Training

After the initial procedure learning, rats were trained to discriminate between a highly similar odor mixture pair. Training on the similar odor discrimination task, $S+$ 1-heptanol 1-octanol 40% : 60% ($\%vol/vol = 0.001$) versus $S-$ 1-heptanol 1-octanol 50% : 50% ($\%vol/vol = 0.001$), followed the procedures described in previous section

(section 2.3.2.4).

Two Doric laser light sources were connected to the optogenetic cannulae inserted in the LC area bilaterally. Light sources were Laser Diode Fiber Light Source: 1-channel model. The central wavelength of light was $473nm$ (blue light) with a power of $90mW$ when coupled into a $400\mu m$ core, NA 0.48 optical fiber. $90mW$ power is the power produced by $150mA$ of current. Each laser light source was connected to a Mono Fiber-optic Patch Cord (Glass, $0.48NA$, $400/430\mu m$) via an FC connector. Fiber-optic patch cords were connected to the two-ferrule cannula via zirconia mating sleeves ($1.25mm$ ferrule diameter) with a black cover. The black cover was used to reduce the laser light reflection.

The two laser light sources were connected with a BNC cable, to have the same light pattern, and both were connected to a computer controlled with Doric software. $10s$, $473nm$ blue light pulses were phasically given to the LC every $30s$ with $10Hz$ pulse frequency and a $30ms$ pulse width.

Rats were trained over days until the $> 80\%$ learning criterion was achieved in two consecutive days.

2.3.2.6 Statistics

OriginPro 9.0 software was used to analyze all datasets. ANOVA among sessions, Tukey post hoc tests and t-tests between the AAV-ChR2 and control groups were used for statistical comparisons. Data are presented as $mean \pm SEM$.

2.3.3 Mobility Effect

To identify the effects of various light patterns, including tonic and phasic stimulation on locomotor activity and arousal, we stimulated LC neurons in the open field box described in section 2.3.2.3 with different light trains and measured changes in their general locomotor activity during light stimulation.

2.3.3.1 Subjects

Subjects were ten AAV injected and five control TH-Cre rats, approximately seven months old at the time of the experiment. Animals were housed under a standard light/dark cycle in single cages with *ad libitum* food and water.

2.3.3.2 Light Parameters Tests

To examine the role of LC-NE neurons in locomotor activity, we selectively light stimulated LC neurons in an open field behavioral test and assessed the rat’s overall mobility. Animals were placed in the behavioral chamber (described in section 2.3.2.3) for a 10min baseline without light. The patchcord was hooked up to their head during the baseline activity. Following the baseline, the laser light was turned on, and light pulses were given to LC neurons for the next 10min of testing.

Testings were performed on animals in a random order on consecutive days. The phasic light pattern was a train of 10s, 473nm blue light pulses given every 30s with a 10Hz pulse frequency and 30ms pulse width. For the tonic testing, two patterns of light were applied with 3Hz or 10Hz tonic light both with 30ms pulse width. To assess any effect, total distance traveled (m) as well as mobility time (s) were

measured by ANY-maze software.

2.3.3.3 Statistics

OriginPro 9.0 software was used to analyze all datasets. For each animal, data was normalized to its own baseline by dividing the testing calculated number by the counted number in the baseline. Two samples t-tests were run to compare AAV-ChR2 and control groups.

2.3.4 Histology

To identify photoactivated neurons and effectiveness of photostimulation, we applied long-term stimulation to visualize photoactivated cells by the immediate early gene (IEG) NPAS4. The light stimulation protocol was the same as during behavioral training $10Hz$ phasic, applying $10s$ of $10Hz$ light pulses with a $30ms$ pulse width every $30s$, for $30min$.

The stimulation was done unilaterally to the left LC in AAV-ChR2 injected and control rats. The non-activated side was considered as a control for each rat. Following a $30min$ time window post light stimulation, rats were transcardially perfused with ice-cold 0.9% saline solution and ice-cold fixative 4% PFA. Brains were removed and stored at $4^{\circ}C$ in 4% PFA for 24 hours and then immersed in 20% sucrose solution for another 24 hours at $4^{\circ}C$ and stored under the same conditions until sectioning. Sectioning, Nissl staining and DBH staining were done as described in section 2.1.4.

For NPAS4 immunohistochemistry, adjacent free-floating sections of LC were washed in Tris buffer (0.1M, pH 7.6) at $5min$ intervals ($\times 3$) to remove remaining PVP solution. Sections then were washed in 1% Hydrogen Peroxide for $30min$ fol-

lowed by three *5min* washes in Tris buffer, Tris A (0.1% Triton X in Tris buffer), and Tris B (0.1% Triton X and 0.005% BSA in Tris buffer). Sections were then incubated in 10% normal goat serum (Sigma-Aldrich, Inc. St. Louis, MO, USA) in Tris B, for *60min* as a blocking buffer to reduce non-specific immuno-staining; followed by two 10 min washes in Tris A and Tris B. Sections were then incubated in NPAS4 antibody (Thermo Fisher Scientific Inc., Carlsbad, CA, USA) at a 1:500 in Tris B for two days in a 4 °C humidified chamber.

On the second day of the procedure, sections were first washed in Tris A and Tris B, each for *10min* and were next incubated in goat anti-Rabbit antibody (Vector Laboratories, Burlingame, CA, USA) diluted 1:1000 in Tris B for *45min* followed by two *10min* washes in Tris A and Tris D (0.1% Triton X and 0.005% BSA in 0.5M Tris Buffer). Sections were then incubated in ABC elite (avidin-biotin horseradish peroxidase complex - Vector Labs) at 1:1000 dilution in Tris D for two hours. Following three *5min* washes in Tris Buffer, sections were incubated in Vector SG peroxidase substrate (Vector Laboratories, Burlingame, CA, USA) for 3 – 7 minutes until sufficient staining had occurred. For free-floating sections, this step was *4min*. When sufficient staining had occurred, sections were washed in distilled water (approximately 5 seconds) to stop the reaction and immediately were moved to Tris Buffer wells for three *5min* washes. Sections were mounted on slides and coverslipped with permount.

In all steps, sections were transferred to new wells by brush. Slides were stored at 4 °C until dried and imaged with a BX-2 brightfield microscope, at 40× magnification.

Chapter 3

Results

3.1 In Vivo Electrophysiology Recording

To examine the effect of various patterns of light on LC firing rate, we performed acute *in vivo* electrophysiology in LC cells of anesthetized rats. Different parameters were applied to identify an effective light pattern for stimulating LC. Each light sequence lasted for 10s and was separated by at least two-minute intervals allowing the cell to return to its baseline activity.

In the AAV-ChR2 infused animals, 10s photostimulation of LC with a 10Hz light frequency and a 30ms pulse width with a 150mA current, significantly increased firing rate from $3.16 \pm 2.54\text{Hz}$ ($M = 3.16$, $SD = 2.54$) preceding the photostimulation to $7.61 \pm 6.15\text{Hz}$ during the light and returning to baseline at $2.37 \pm 2.00\text{Hz}$ following the light train. The response of this subset of N=6 cells was analyzed statistically through One-way repeated measures ANOVA. Results showed a significant increase in LC firing during this pattern of light, $F(2, 10) = 8.69$, $p = 0.03$ (Figure 3.1A).

Further analysis through Tukey post-hoc tests for pairwise comparisons, confirmed this significant activation of LC cells by comparing LC firing during the light, to that of the 10s time period pre-light, $p = 0.02$ and post-light, $p = 0.008$. The firing rate of cell 10s post-light and 10s pre-light are not different significantly, $p = 0.83$.

Figure 3.1B shows the effect of the same light except for pulse width. This light train is 10s, 10Hz, 150mA with a 50ms pulse width. There is a significant increase from $3.70 \pm 2.38Hz$ as baseline preceding the light to $9.28 \pm 4.84Hz$ during photostimulation and decreasing to baseline at $2.23 \pm 2.23Hz$ following the light. One-way repeated measures ANOVA, analyzing the data obtained from this subset of N=6 cells from 3 animals reveals a significant increase in LC firing during this pattern, as well, $F(2, 10) = 25.42$, $p = 0.0001$.

Tukey post-hoc analysis for comparing each time interval to one another confirmed the significant activation of LC cells. Photostimulation caused a significant increase in firing rate in comparison to pre-light baseline activity, and post-light, $p < 0.001$ in both. Also, there is no significant difference between cell firing before and after light stimulation $p = 0.37$.

However, by changing the light source power via changing the current to 100mA, in a 10Hz, 30ms light train, although light stimulation increases the firing rate, this effect is not significant, $p > 0.1$. In this subset of N=4 cells, as shown in Figure 3.1C, firing rate was increased from $1.2 \pm 1.13Hz$ preceding the light to $2.65 \pm 3.15Hz$ during the light and decreased to baseline at $1.05 \pm 1.35Hz$ post-light.

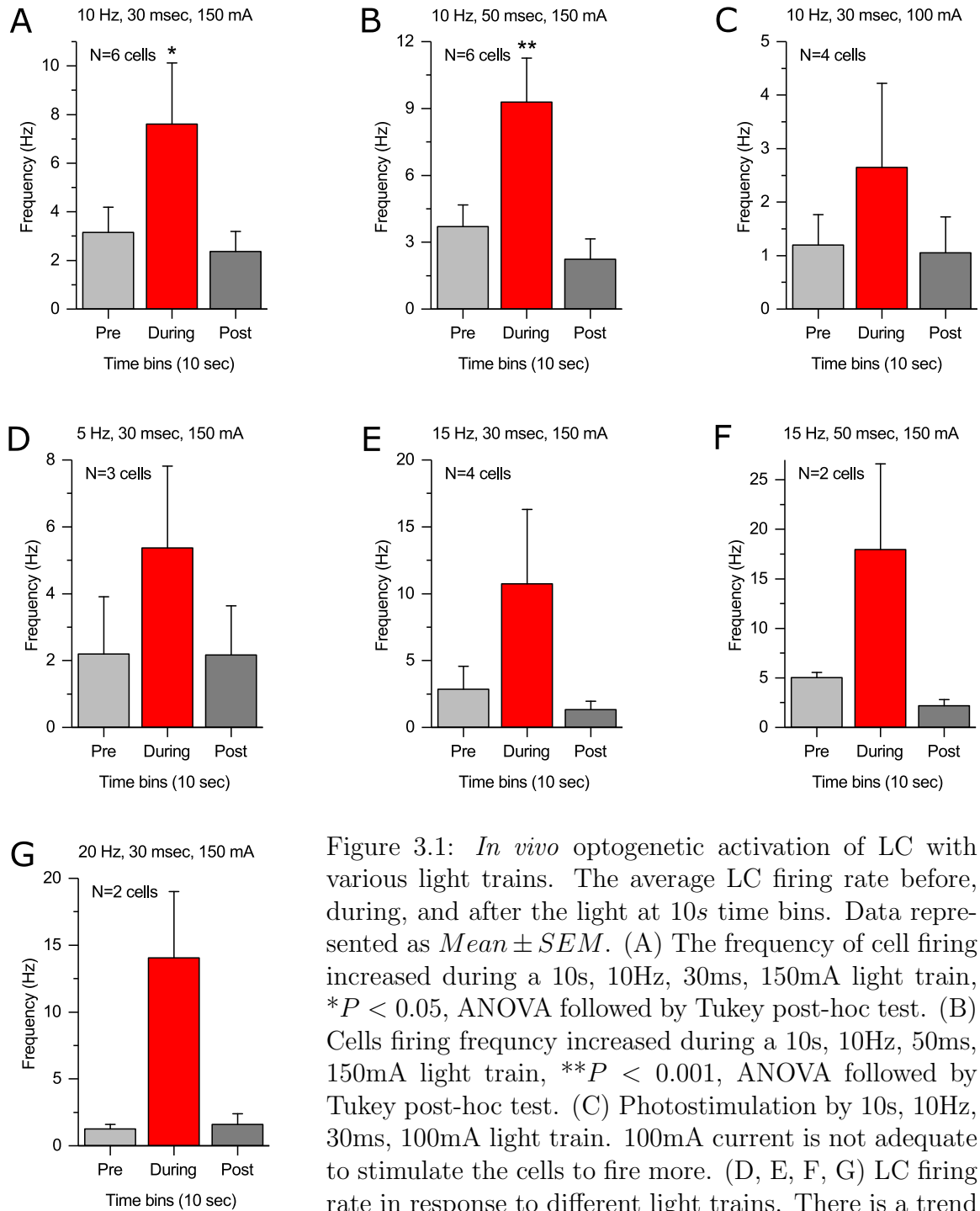


Figure 3.1: *In vivo* optogenetic activation of LC with various light trains. The average LC firing rate before, during, and after the light at 10s time bins. Data represented as $Mean \pm SEM$. (A) The frequency of cell firing increased during a 10s, 10Hz, 30ms, 150mA light train, $*P < 0.05$, ANOVA followed by Tukey post-hoc test. (B) Cells firing frequency increased during a 10s, 10Hz, 50ms, 150mA light train, $**P < 0.001$, ANOVA followed by Tukey post-hoc test. (C) Photostimulation by 10s, 10Hz, 30ms, 100mA light train. 100mA current is not adequate to stimulate the cells to fire more. (D, E, F, G) LC firing rate in response to different light trains. There is a trend of response; however, the effect is not significant.

We further tested various light pulse frequencies. Figure 3.1D shows decreasing the frequency down to $5Hz$ with maximum current ($150mA$) and $30ms$ pulse width, led to a non-significant increase from $2.2 \pm 2.96Hz$ preceding the light to $5.37 \pm 4.25Hz$ during the light and returning to $2.17 \pm 2.55 Hz$ post-light in a subset of $N=3$ cells, $p = 0.10$.

Similarly, in a subset of $N=4$ cells, increasing the pulse frequency to $15Hz$, with other parameters intact, resulted in a non-significant change from $2.85 \pm 3.47 Hz$ pre-light to $10.74 \pm 11.10 Hz$ during the light and returning to $1.34 \pm 1.22 Hz$ post-light, $p = 0.15$. (Figure 3.1E)

The same trend was observed with the same light with wider pulses ($50ms$ pulse width). In the subset of $N=2$ cells, photostimulation caused an increase from $5.03 \pm 0.74 Hz$ as baseline activity to $17.95 \pm 12.23 Hz$ in response to light and returning to baseline at $2.18 \pm 0.88 Hz$ post-light. (Figure 3.1F).

We also tested the effect of very high light frequency in $N=2$ cells. Light pattern was applied at the rate of $20 Hz$ with $30ms$ pulses, $150mA$ current, which caused an increase from $1.25 \pm 0.5 Hz$ preceding the light to $14.05 \pm 7.0 Hz$ during the light and returning to the baseline firing $1.6 \pm 1.13 Hz$ following light activation. (Figure 3.1G).

As Figure 3.1 shows, the $10Hz$ light stimulations significantly increased the LC firing rate. Our data was significant with $N=6$ cells in both $10Hz$, $30ms$, $150mA$ and $10Hz$, $50ms$, $150mA$ patterns. At other frequencies, we observed a trend of increased LC firing during light, but the data did not reach statistical significance, likely due to the small sample rate and/or higher variability. We selected $30ms$ pulse width for our behavioral experiments since the data suggested a greater suppression

after photostimulation with the 50ms pulse width light (Figure 3.1B).

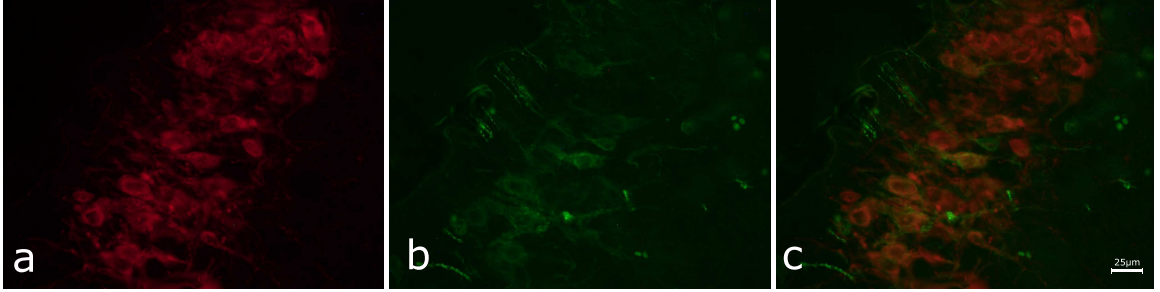


Figure 3.2: Average AAV expression in LC cells. (a) LC neurons identified by DBH staining, (b) Average virus (GFP+) expression in LC cells, (c) Overlap of DBH+ and GFP+ cells

To confirm the expression of ChR2 in LC cells, we looked at the virus expression in rats that were stimulated. If the optical fiber placement was beyond the boundaries of LC, the animal was removed from all the calculations. Three rats were excluded at this stage.

Figure 3.2 shows the average virus expression in LC cells. Immunohistochemical analysis of the LC sections at a minimum of four-weeks post-infusion revealed GFP expression (the indicator of the virus) within the range of DBH positive cells (the indicator of LC cells). To obtain the percentage of DBH+ cells expressing GFP for each subject, colocalization counts were completed. For $N = 4$ tissues, the average percentage of GFP expression over DBH+ cells was $68.2 \pm 8.4\%$ for the LC-ChR2 channel-activated subjects.

3.2 Learning Promoting Effect

In order to test the involvement of the LC in odor discrimination learning, AAV-ChR2(h134r) was bilaterally infused in TH-Cre rats. Age-matched control rats were not infused with the virus. Both AAV-ChR2 (N=7) and control (N=7) groups were then implanted with optical fibers and underwent training.

After habituation, rats were trained in an initial procedure learning task. Discrimination learning was defined as 80% correct responses in two consecutive days. Figure 3.3 shows all animals learned to discriminate between two simple odors within six days. They started from $30 \pm 24\%$ correct response and reached $81 \pm 11\%$ on the 6th day and improved to $86 \pm 9\%$ on the 7th day.

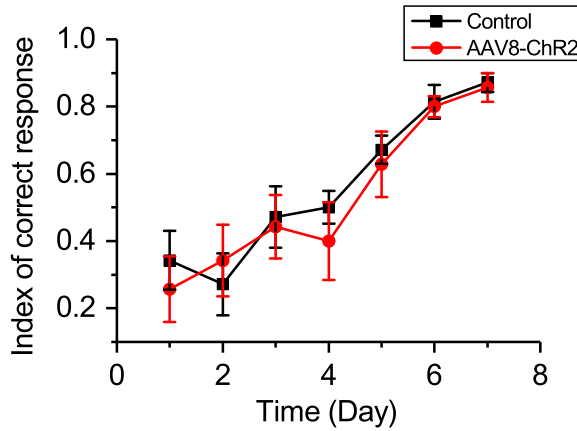


Figure 3.3: Index of correct responses in simple odor discrimination training. Correct responses in the AAV-ChR2 and control groups over seven days of training.

A test of two-way ANOVA over all N=14 animals shows that their number of correct responses differed significantly over the days ($F(6, 84) = 16.84$, $p < 0.0001$) in both AAV-ChR2 and control groups. Tukey post-hoc tests reveal that correct

responses from days 5-7 were significantly better than those on days 1 and 2, $p < 0.0001$. AAV-ChR2 and control groups' acquisition does not differ significantly, $p = 0.47$.

Their latency to the first nose poke decreased over days from $142.35 \pm 34.64s$ on the first day to $59.5 \pm 37.48s$ on the 7th day, (Figure 3.4) showing that animals are actually learning the procedure of training. A test of two-way ANOVA reveals that AAV-ChR2 injected and control animals are not different in the latency to respond, $p = 0.18$, and both AAV-ChR2 and control groups were improving over the training days ($F(6, 84) = 8.23$, $p < 0.0001$). For pairwise comparisons, Tukey tests show animals' latency to respond, significantly decreased from day 1 to day 6, $p < 0.001$.

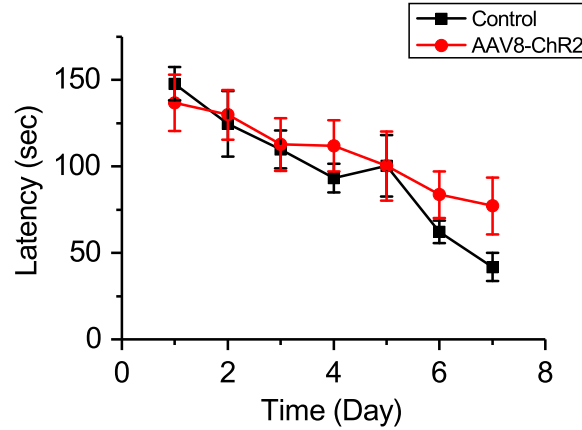


Figure 3.4: Latency to respond in simple odor discrimination training. Latency to respond in the AAV-ChR2 and control groups over seven days of training.

These data indicate all rats learned the procedure. Following simple odor discrimination acquisition, rats were trained to discriminate between two highly similar odor mixtures. Two experimental animals were removed from the experiment since their cement cap holding the optical fiber detached. Thus, N=5 AAV-ChR2 and N=7 con-

trol rats were included in the next experiment's data. Animals were photostimulated during the experiment with a phasic $10Hz$ light with $30ms$ pulses for a duration of $10s$, every $30s$.

Figure 3.5 shows the promoting effect of LC light activation on the ability of AAV-ChR2 infused animals to perform a highly-similar odor discrimination task, in comparison to controls. AAV-ChR2 rats started from $56 \pm 30\%$ on the first day and learned to discriminate 80% correctly with an index of $80 \pm 7\%$ on the 3rd day. Meanwhile, control animals started from $54 \pm 21\%$ on day 1 and reached $46 \pm 16\%$ on day 3. The training was continued until control animals could discriminate correctly in at least 80% of their choices in two consecutive days. On day 8, control animals reached learning criteria.

As Figure 3.5 represents, control animals learned the discrimination gradually and reached the percentage of $81 \pm 7\%$ on day 8 while AAV-ChR2 animals are at the level of $92 \pm 8\%$ on this day. Learning was persistent until the experiment ended on day 10 with indexes of $92 \pm 8\%$ correct in the AAV-ChR2 and $83 \pm 15\%$ in the control group.

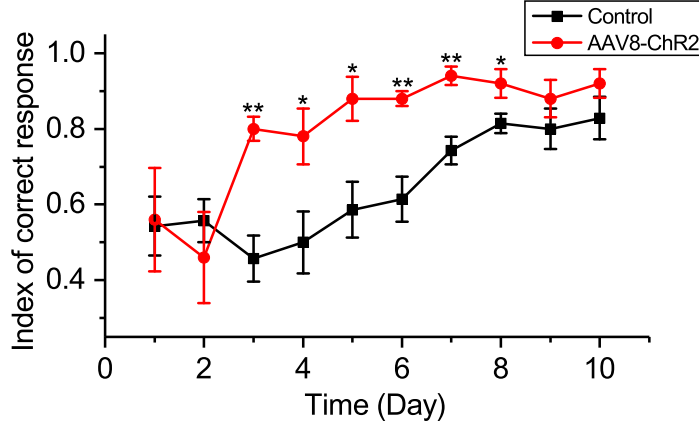


Figure 3.5: Index of correct responses in difficult odor discrimination training. Correct responses in the AAV-ChR2 and control groups over ten days of training; 10s, 10Hz, 30ms, 150mA light pulses are given every 30s. * $p < 0.05$, ** $p < 0.01$.

The overall effect of light was significant as shown in a two-way ANOVA test. The AAV-ChR2 and control groups have significantly different patterns of learning, $F(1, 100) = 28.65$, $p < 0.001$. Animals' correct responses increased significantly over time in both groups, $F(9, 100) = 8.36$, $p < 0.001$; and the overall effect of stimulating LC in the daily learning procedure (interaction) was also significant, $F(9, 100) = 2.29$, $p = 0.02$. Tukey post-hoc test shows the effect was significant by comparing AAV-ChR2 and control groups, $p < 0.0001$.

Follow-up two-sample t-tests, comparing AAV-ChR2 and control animals, confirms photostimulation prompted a significant difference in correct response from day 3 on ($t(10) = 4.40$, $p = 0.001$ on the 3rd day, and $p < 0.05$ on days 4-8, Figure 3.5).

In Figure 3.6, animals' latency to respond is presented as an index of motivation. A test of two-way ANOVA shows they chose significantly faster over the training days, $F(9, 100) = 5.33$, $p < 0.001$; and there is no difference between AAV-ChR2 and

control groups, $p = 0.30$. They started from $77.83 \pm 50.58s$ and reached $20.92 \pm 16.32s$ on the 10th day.

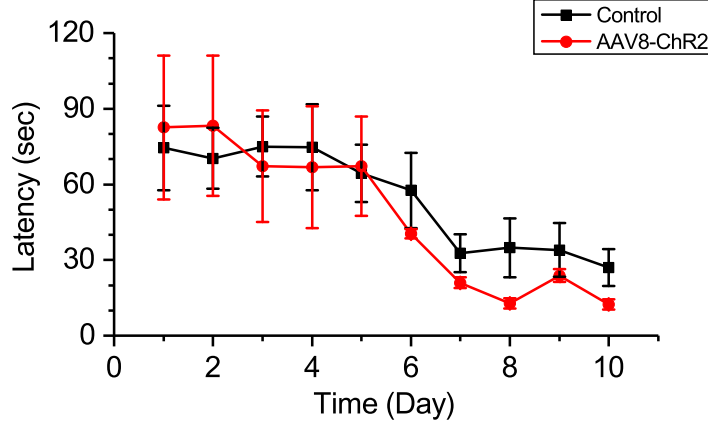


Figure 3.6: Latency to respond in difficult odor discrimination training. Latency to respond in the AAV-ChR2 and control groups over ten days of training; 10s, 10Hz, 30ms, 150mA light pulses are given every 30s.

3.3 Mobility Effect

NE neurons of the LC-NE system naturally fire in distinct modes in response to various environmental challenges, as follows: (1) low tonic 1 – 3Hz LC discharge which is consistent with an awake state (Carter et al., 2010, 2012); (2) high tonic 3 – 8Hz firing in stressful events and stimuli (Reyes et al., 2008; Curtis et al., 2012); (3) phasic burst 8 – 10Hz firing in response to sensory stimuli, such as touch, flashes of light, auditory tones (McCall et al., 2015; Aston-Jones & Bloom, 1981b; S. Foote et al., 1980).

We studied the effects of LC photostimulation using three different light patterns to see whether the pattern of stimulation modulates any change in animal’s general

activity. Low and high tonic stimulation consisted of constant $30ms$ light pulses at $3Hz$ and $10Hz$, whereas phasic stimulation consisted of $30ms$ pulses at $10Hz$ for $10s$ every $20s$, the same as the odor discrimination light trains.

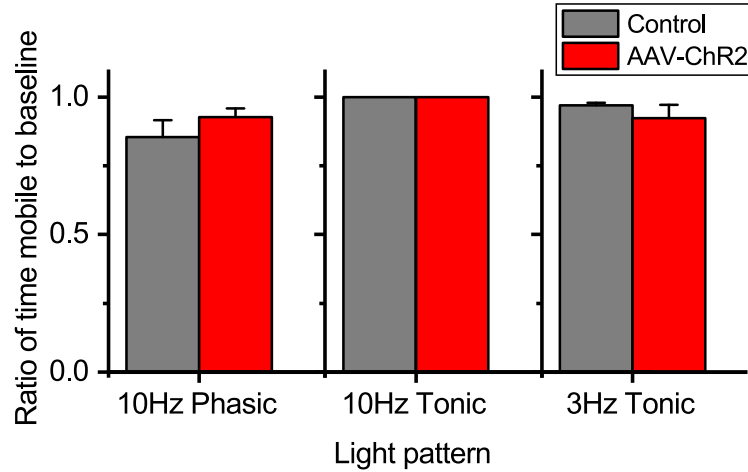


Figure 3.7: Ratio of mobility time during photostimulation at different light frequencies to the baseline

We examined the rats' mobility time in each time period during the $10min$ baseline and $10min$ light stimulation, as well as the total distance travelled as indicators of general locomotor activity. Figure 3.7 shows the ratio of mobility time during photostimulation to the baseline in AAV-ChR2 and control animals. Two sample t-tests comparing AAV-ChR2 and control animals show different stimulation patterns had not differentially affected rats mobile time ($p > 0.1$).

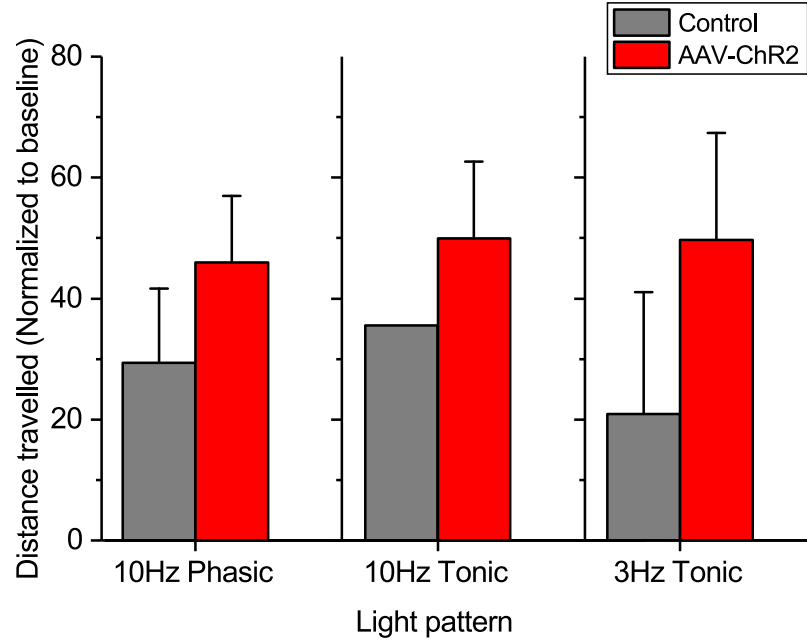
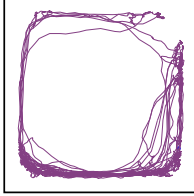
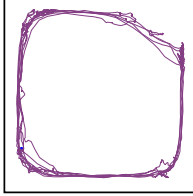
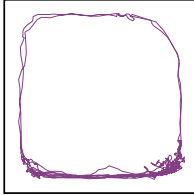
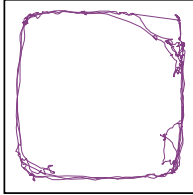
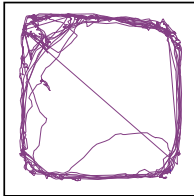
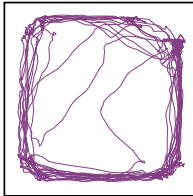
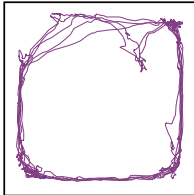
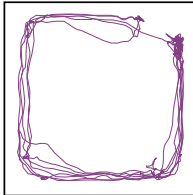
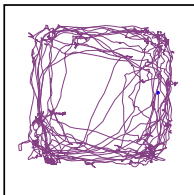
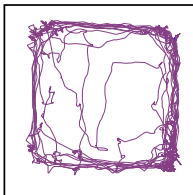
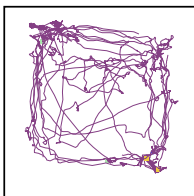



Figure 3.8: Ratio of distance travelled during photostimulation at different light frequencies to the baseline

Similarly, the ratio of total distance travelled during photostimulation to baseline was calculated and is shown in Figure 3.8. Two sample t-tests reveal that there is no significant difference in animals' total activity between AAV-ChR2 infused and control groups ($p > 0.1$). All numbers are calculated by ANY-maze behavioural tracking software.

Table 3.1 provides examples of tracking animal movements by ANY-maze. Each graph is from one animal, comparing photostimulation activity to baseline. The data suggests that LC photostimulation does not affect rats' general locomotor activity. Following all behavioral experimental procedures, the same light stimulus as the behavioral pattern was applied to the LC for 30min (10Hz phasic 10s with 30ms pulse width every 30s).

Table 3.1: Examples of tracking rats' bodies in the open field mobility test

	AAV-ChR2 Infused	Non-infused Control
Baseline		
Phasic 10Hz, PW 30ms for 10s every 30s		
Baseline		
Tonic 3Hz, PW 30ms		
Baseline		
Tonic 10Hz, PW 30ms		

Animals were placed in the open field box for a 10min baseline without light. The patch cord was hooked up to their head during the baseline activity. Following the baseline, light pulses were given to LC neurons for the next 10min testing.

The stimulation was done unilaterally to the left LC in AAV-ChR2 injected and control rats. The non-activated side was considered as a control for each rat. Following a 30 min time window post light stimulation, rats were transcardially perfused and tissue was processed for Npas4 immunoreactivity in LC neurons. Figure 3.9 shows photostimulation increases Npas4 immunoreactivity in LC neurons.

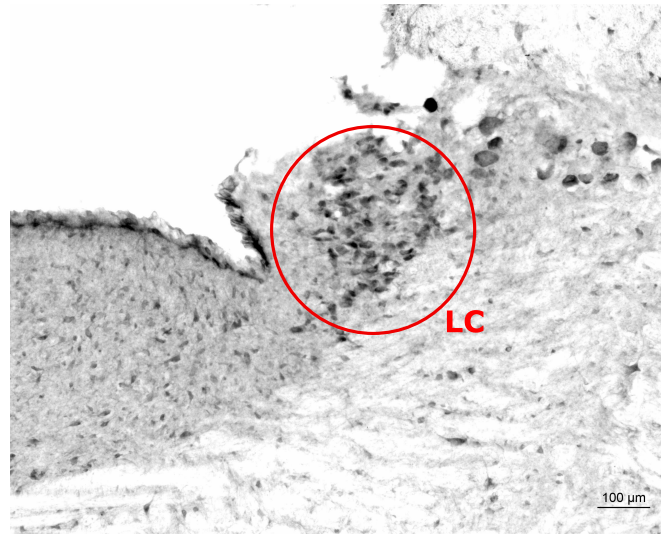


Figure 3.9: Npas4 immunoreactivity in LC neurons. Dark spotted cells are activated LC cells in each section.

Chapter 4

Discussion

4.1 Summary of Major Findings

The purpose of this research was to investigate the effect of putative enhanced LC-NE release as a result of LC phasic activation on odor discrimination learning in adult rats. With the optogenetic manipulation of LC, we first investigated the effect of various patterns of photostimulation on LC activity, *in vivo*. We also aimed to gain insight into whether these different firing rates of the LC neurons affect general locomotor activity.

To this aim, adult rats were first infused with the viral construct containing the light-activated channel. Immunohistochemical analysis of the LC sections at a minimum of four-weeks post-infusion revealed robust, selective GFP expression (the indicator of the viral construct) within DBH positive cells (the indicator of LC cells). The average percentage of GFP expression over DBH positive cells was $68.2 \pm 8.4\%$ for the LC-ChR2 channel-activated subjects.

We performed *in vivo* recording to identify an effective light pattern for activating LC neurons. Blue light with a central wavelength of $473nm$ and a power of $90mW$ was delivered via fiber-optic patch cords to the LC cells. Various light patterns were tested. $10Hz$ light trains significantly increased the LC firing rate in both $10Hz$, $30ms$, $150mA$ and $10Hz$, $50ms$, $150mA$ patterns. At other frequencies, we observed a trend of increased LC firing during light, but the data did not reach statistical significance. We selected the $30ms$ pulse width for our behavioral experiments since data suggested a greater suppression after photostimulation with the $50ms$ pulse width light.

Another cohort of rats was then trained to an odor discrimination task with the selected light pattern given to the LC. Three weeks or later following the infusions, we implanted animals with the optogenetic cannulae to permit the bilateral photostimulation of the LC. Age-matched control rats were also implanted with cannulae at the same time.

Based on the result obtained from *in vivo* recordings, these cohorts were also tested for potential mobility and general locomotor activity changes as a response to the light stimulation. Patterns included low tonic $3Hz$, high tonic $10Hz$ and phasic $10Hz$ every $30s$. The immobility time was close to zero in all light patterns, while the distance travelled was not significantly different in AAV-ChR2 injected compared to control animals. Although there is a trend of increased mobility in all cases in AAV-ChR2 animals compared to control rats, the effect is not significant due to the high variability among animals.

They were also trained to the odor discrimination task. Habituation and simple odor discrimination training was performed for all animals and they achieved the

same level of simple odor learning prior to the highly similar task.

Following that, rats were trained to a highly similar odor discrimination task in which a 10Hz phasic light was given to the LC with 30ms pulse width for 10s every 30ms. AAV-ChR2 infused rats started from $56 \pm 30\%$ on the first day and learned to discriminate correctly in $80 \pm 7\%$ of their choices on the 3rd day. Meanwhile, control animals started from $54 \pm 21\%$ on day 1 and reached $46 \pm 16\%$ on day 3. The training was continued until control animals could discriminate correctly in at least 80% of their choices in two consecutive days. On day 8, control animals reached $81 \pm 7\%$ of correct responses. The overall effect of light over the days of training was significant. This shows the promoting effect of light on the ability of AAV-ChR2 infused animals to perform a highly-similar odor discrimination test, in comparison to control rats. The induced LC-NE activity by photostimulation appeared to have facilitated attention to the specific inputs and to have increased the rate of acquisition of the discrimination task.

4.2 In Vivo Electrophysiology Recordings

4.2.1 Light Patterns for LC Activation

In the initial stages of this research, we tried various manipulations of stimulation parameters to identify an effective light pattern for LC photostimulation for use in the behavioral experiments. Each light train has four parameters: Frequency (Hz), pulse width (ms), current (mA) (affects the power of light) and light duration described as the number of pulses per sequence.

Through experimentation on confirmed LC neurons in the electrophysiological setup, we found that the most reliable pulse widths for activating LC neurons are $30ms$ and $50ms$. Pulses with a width less than $30ms$ were too short to produce activation of LC neurons. On the other hand, $50ms$ pulse widths and more became less reliable than $30ms$ pulses when used in trains of lights or sequences. These higher intensities appeared to cause a trend of suppressions post-stimulation, which we did not want in our behavioral experiments.

Moreover, multiple frequencies were similarly tested. This includes light trains of $1Hz$, $1.5Hz$, $5Hz$, $10Hz$, $15Hz$, $20Hz$ and $30Hz$. The lower frequencies did not activate LC neurons, while the $5Hz$ and higher frequencies could elicit a response from LC neurons. However, the trend was not significant in all cases which can be due to the small number of cells included in the statistical analyses. On the other hand, higher frequency light trains showed a trend of suppressing cells after long phasic trains. This was in accordance with the mouse study by Carter et al. (2010), that showed that frequencies higher than $5Hz$ enabled LC neurons to activate in response to light.

Intensity power of output light was $90mW$ with corresponding $150mA$ current. We also tested $100mA$ current and observed that the cells response was less robust and consistent with the lower light power resulting from the lower current. Thus, in all of the experiments, we employed the maximum current producing $90mW$ light power. However, in mice studies, lower light powers were able to produce the desired response as reported by Carter et al. (2010) and Hickey et al. (2014), as $20mW$ and $1 - 30mW$, respectively.

$10Hz$ light stimulations significantly increased the LC firing rate. Our data was

also significant with $N=4$ cells in both $10Hz$, $30ms$, $150mA$ and $10Hz$, $50ms$, $150mA$ patterns (See figure 3.1). We selected $30ms$ pulse width for our behavioral experiments since data suggested a greater suppression after photostimulation in $50ms$ pulse width light.

4.2.2 Effect of In Vivo Photostimulation on LC Activation

Due to the nature of the experiment, the number of testings for each parameter of the light pattern was often varied. In two cases, the subjects died during the experiment, so they were removed from reported results and statistics, but the implications that came from the analysis were utilized for the next experiments. In the first recordings, there were more variations of light patterns applied to each subject, and some had filtered out through further experiments. On the other hand, we had to prevent the potential exhaust of neurons that had been stimulated multiple times. Thus, further in the experiments, we tested fewer light trains on each subject.

After each light pattern, sufficient time was allowed for cells to return to their natural baseline firing rate. In the analysis of data, we ensured that these variations would have no effect on the results of each light parameter. If a subject's baseline activity was higher than the normal tonic LC activity, reaching up to $30Hz$ - this was likely due to cells nearby LC being close to the tip of electrode. In these instances, the data was removed from the analysis.

Light trains ranging from $5Hz$ to $20Hz$ were observed to be capable of increasing the firing rate of LC neurons. The effect was acute and specific to the time duration of light stimulation followed by a sharp decrease to the baseline rate of firing. Interest-

ingly, when the light was shone with maximum power ($150mA$ current), it enhanced the LC firing rate close to the level of its own frequency. For instance, a $10s$ train of $10Hz$, $50ms$, $150mA$ pulses, increased the firing rate from $3.70 \pm 2.38Hz$ as the baseline to $9.28 \pm 4.84Hz$ during photostimulation; while a train of $5Hz$, $30ms$, $150mA$ increased neuronal activity from $2.2 \pm 2.96Hz$ preceding the light to $5.37 \pm 4.25Hz$. This trend can be seen in the figure 3.1 with the average activity of cells represented. Overall, the patterns of response in cells with a normal low frequency baseline between $1Hz$ to $5Hz$ were consistent and promising in different stimulation frequencies.

4.3 Behavioral Effects of Optogenetic Stimulation

4.3.1 Light Patterns in Terms of Behavior - Mobility Effect

After confirming several light patterns that could elicit the LC neuronal activity, we investigated the effect of those lights on rats' general behaviors such as potential changes in locomotive activity. It has been shown by Carter et al. (2010) that optogenetic stimulation of the LC neurons in awake-behaving mice regulates their locomotor activity which was dependent on the light pattern as well as the length of the stimulation period to the LC (Carter et al., 2010). They showed that $1h$ tonic stimulation with a $3Hz$, $10ms$ light pulses increases general mobility while phasic stimulation with $10Hz$, $10ms$ light pulses in burst duration of $500ms$ every $20s$ decreases the mice mobility over the hour of stimulation. Our result in rats shows that different patterns of stimulation do not have a significant effect on rats' general mobility over the $10min$ of stimulation. They observed reversible behavioral arrest

in sustained high-frequency stimulations of $5Hz$ to $25Hz$ with 100% probability in $15Hz$ and more.

We used more powerful light, with longer pulse width, but less total duration. Patterns were low tonic $3Hz$, high tonic $10Hz$ and phasic $10Hz$ every 30s. The immobility time was close to zero in all light patterns, while the distance travelled was not significantly different in AAV-ChR2 injected compared to control animals. Although there is a trend of increased mobility in all cases in AAV-ChR2 animals compared to control rats, the effect is not significant due to the high variability among animals.

In the phasic mode, the LC has a burst of activity, which is thought to be driven by decision processes in response to a specific task and by novel input. This burst of firing produces a broad release of NE, increasing the gain of cortical processing units and facilitating task-relevant behavior (Aston-Jones & Cohen, 2005). In other words, the burst of firing is specific to the event, facilitating the corresponding processes, thereby increasing the performance of the current task relative to other distracting events (Aston-Jones & Cohen, 2005). On the other hand, the tonic firing mode increases the baseline NE release, which increases sensitivity of target neurons to a wider range of environmental events and in a stressful situation, helps the animal to attend to a broad variety of surrounding events (Aston-Jones & Cohen, 2005).

In our behavioral mobility testings, rats were completely habituated to the chamber and behavioral setup. The testings were done in an open field box. Thus, when there is no actual environmental stimuli (endogenous phasic burst) or stressful situation (endogenous high tonic), cortical networks might correct the NE release via feedback connections and there would be no change in general mobility as the result

of the external light stimulation. Our results provide data consistent with the recent study published by Vazey et al. (2018) that reported phasic, but not tonic, LC firing generated salience in sensory neurons and these LC-induced salience signals occurred without changes in arousal.

All in all, for our purpose of establishing side effects of light on animal’s activity, we did not observe a significant difference between utilized light patterns.

4.3.2 Effect of LC Photostimulation on Promoting Learning

In the highly similar odor discrimination setup, both AAV-ChR2 cohort and control rats were light stimulated to make all environmental distractions and the possible heating effect of light similar. AAV-ChR2 channel infused rats could discriminate the similar odors after 3 days of training, while non-infused control rats reached the learning criteria in 8 days. The enhanced LC activity by light stimulation during highly similar odor discrimination training induced faster learning.

It has been shown that rats infused directly with additional NE into the OB, in a non-associative and spontaneous paradigm detected and discriminated odors at lower thresholds of concentrations (Escanilla et al., 2010). In motivational reward learning, studies show that blockade of bulbar NE receptors slows odor responses (Doucette et al., 2007; Mandairon et al., 2008; Escanilla et al., 2012; Shakhawat et al., 2015). These results confirm a critical role for NE in olfactory processing and learning, particularly in discrimination tasks. In our experimental setup, the enhanced LC activity by light stimulation during highly similar odor discrimination training induced faster learning. Our result is consistent with previous experiments showing that OB NE facilitates

similar odor discrimination.

LC firing rate varies in response to different environmental conditions. Low-frequency tonic firing is active as a background firing during everyday behaviors, which is a slow, rhythmic pattern around $1 - 3Hz$, and is consistent with an awake state (Carter et al., 2010, 2012), while in a stressful environment the tonic firing rate increases to $3 - 8Hz$ (Reyes et al., 2008; Curtis et al., 2012) and can be as high as $15Hz$ for a limited duration, under high arousal conditions (Berridge & Waterhouse, 2003). Optogenetic stimulation of LC with a high tonic light pattern is reported to initiate anxiety-like as well as aversive behaviors, in mice (McCall et al., 2015).

On the other hand, in response to sensory stimuli, phasic bursts of firings are active that have typically $8 - 10Hz$ firing rate (McCall et al., 2015; Aston-Jones & Bloom, 1981b). This mode is active in decision-making processes for a specific environmental task (Aston-Jones & Cohen, 2005). In our experiments of difficult odor discrimination training, we photostimulated LC with a $10Hz$ phasic light pattern consistent with endogenous phasic bursts. This induced activity by photostimulation facilitated the temporal attention to the specific event and increased the performance of the discrimination task relative to other distracting environmental events.

4.4 Conclusions and Future Directions

This research was an exploration into the effect of the phasic activity mode of LC on learning. We have established a promising result from *in vivo* LC stimulation and recordings and utilized an effective light pattern obtained from *in vivo* recording experiments in awake behaving rats. We phasically photostimulated LC neurons to

gain insight into how enhanced burst firing of the LC can modulate learning in a highly similar odor discrimination task.

A potential future direction for this research would entail replicating these findings with additional subjects. This would assess promising outcomes from the results which did not reach statistical significance due to small sample size, but had noticeable trends.

We have established the learning effect with the phasic light pattern. The next step is to modify the behavioral paradigm and test the effect of tonic light patterns; as high tonic LC firing mode is reported to drive anxiety-like behaviors, the effect might slow down the learning.

It is also of interest to investigate the effect of LC photostimulation on dopamine circuitries. This can be done as an experiment using a place preference test. Kempadoo et al (2016) tonically photostimulated the LC-to-hippocampus catecholamine axons to investigate this effect. Their result shows that dopamine signaling in the dorsal hippocampus is not an inherently reinforcing or rewarding signal and photostimulation had no effect on their conditioned place preference test, in mice (Kempadoo, Mosharov, Choi, Sulzer, & Kandel, 2016). The light pattern in this experiment was a $20Hz$ light with $5ms$ pulses continuously. On the other hand, it has been reported by McCall et al. (2015) that high tonic photostimulation generates anxiety-like behavior in mice. Thus, it would be of interest to design a place preference test utilizing various light patterns and observe the potential effects. In the final stages of this research, we have started piloting a conditioned place preference test with preliminary results. The result of such experiment merged with what this research focused on, would provide insight into the interaction on LC-NE and DA systems. This potential

would provide an understanding of how disruptions in the LC-NE and DA systems contribute to the complex patterns of behavior.

Chapter 5

Conclusions

The primary purpose of this research was to investigate the effect of phasic photostimulation of LC on odor discrimination learning in adult rats. With the optogenetic manipulation of LC, we first investigated the effect of various patterns of photostimulation on LC activity, *in vivo*. We also aimed to gain insight into how these different firing rates of the LC neurons modulate general locomotive activity.

We performed *in vivo* recording to identify effective light patterns for activating LC neurons. A blue light at a power of $90mW$ and a central wavelength of $473nm$ was illuminated via fiber-optic patch cords to the LC cells. Various light patterns were tested. $10Hz$ light trains with $30ms$ and $50ms$ pulse width significantly increased the LC firing rate when maximum power was utilized.

Another cohort of rats was then trained to an odor discrimination task with the selected light pattern given to the LC. Based on the result obtained from *in vivo* recordings, rats were tested for potential mobility changes. Patterns included low tonic $3Hz$, high tonic $10Hz$ and phasic $10Hz$ every $30s$ all with $30ms$ pulse width.

The immobility time was close to zero in all light patterns, while the distance travelled was not significantly different in AAV-ChR2 injected compared to control animals.

Rats were finally trained to the odor discrimination task. Habituation and simple odor discrimination training were carried out for all animals and they all reached the same learning criterion for the initial simple discrimination. Following that, rats were trained to a highly similar odor discrimination task in which a $10Hz$ phasic light was given to LC with a $30ms$ pulse width for $10s$ every $30ms$. AAV-ChR2 infused rats learned to discriminate correctly in more than 80% of their choices on the 3rd day of the training, while, control animals reached this criteria on day 8. The overall effect of light over the days of training was significant. We suggest the enhanced LC activity by optical stimulation during the highly similar odor discrimination training induced faster learning via modulation of plasticity and facilitated attention.

References

- Aghajanian, G. K. (1978). Tolerance of locus coeruleus neurones to morphine and suppression of withdrawal response by clonidine. *Nature*, 276(5684), 186.
- Aston-Jones, G., & Bloom, F. (1981a). Activity of norepinephrine-containing locus coeruleus neurons in behaving rats anticipates fluctuations in the sleep-waking cycle. *Journal of Neuroscience*, 1(8), 876–886.
- Aston-Jones, G., & Bloom, F. (1981b). Nonrepinephrine-containing locus coeruleus neurons in behaving rats exhibit pronounced responses to non-noxious environmental stimuli. *Journal of Neuroscience*, 1(8), 887–900.
- Aston-Jones, G., & Cohen, J. D. (2005). Adaptive gain and the role of the locus coeruleus–norepinephrine system in optimal performance. *Journal of Comparative Neurology*, 493(1), 99–110.
- Belluscio, L., Lodovichi, C., Feinstein, P., Mombaerts, P., & Katz, L. C. (2002). Odorant receptors instruct functional circuitry in the mouse olfactory bulb. *Nature*, 419(6904), 296.
- Berridge, C. W., & Waterhouse, B. D. (2003). The locus coeruleus–noradrenergic system: modulation of behavioral state and state-dependent cognitive processes. *Brain Research Reviews*, 42(1), 33–84.

- Camp, L. L., & Rudy, J. W. (1988). Changes in the categorization of appetitive and aversive events during postnatal development of the rat. *Developmental Psychobiology: The Journal of the International Society for Developmental Psychobiology*, 21(1), 25–42.
- Carter, M. E., Brill, J., Bonnavion, P., Huguenard, J. R., Huerta, R., & de Lecea, L. (2012). Mechanism for hypocretin-mediated sleep-to-wake transitions. *Proceedings of the National Academy of Sciences*, 109(39), E2635–E2644.
- Carter, M. E., Yizhar, O., Chikahisa, S., Nguyen, H., Adamantidis, A., Nishino, S., ... De Lecea, L. (2010). Tuning arousal with optogenetic modulation of locus coeruleus neurons. *Nature Neuroscience*, 13(12), 1526.
- Cedarbaum, J. M., & Aghajanian, G. K. (1978). Afferent projections to the rat locus coeruleus as determined by a retrograde tracing technique. *Journal of Comparative Neurology*, 178(1), 1–15.
- Ciombor, K., Ennis, M., & Shipley, M. (1999). Norepinephrine increases rat mitral cell excitatory responses to weak olfactory nerve input via alpha-1 receptors in vitro. *Neuroscience*, 90(2), 595–606.
- Cooke, S., & Bliss, T. (2006). Plasticity in the human central nervous system. *Brain*, 129(7), 1659–1673.
- Curtis, A. L., Leiser, S. C., Snyder, K., & Valentino, R. J. (2012). Predator stress engages corticotropin-releasing factor and opioid systems to alter the operating mode of locus coeruleus norepinephrine neurons. *Neuropharmacology*, 62(4), 1737–1745.
- Dahlstrom, A., & Fuxe, K. (1964). Existence of monoamine-containing neurons in the central nervous system. i. demonstration of monoamines in the cell bodies

- of brain stem neurons. *Acta Physiologica Scandinavica*, 62.
- Devore, S., Lee, J., & Linster, C. (2013). Odor preferences shape discrimination learning in rats. *Behavioral Neuroscience*, 127(4), 498.
- Doty, R. L., Ferguson-Segall, M., Lucki, I., & Kreider, M. (1988). Effects of intrabulbar injections of 6-hydroxydopamine on ethyl acetate odor detection in castrate and non-castrate male rats. *Brain Research*, 444, 95–103.
- Doucette, W., Milder, J., & Restrepo, D. (2007). Adrenergic modulation of olfactory bulb circuitry affects odor discrimination. *Learning & memory*, 14(8), 539–547.
- Escanilla, O., Alperin, S., Youssef, M., Ennis, M., & Linster, C. (2012). Noradrenergic but not cholinergic modulation of olfactory bulb during processing of near threshold concentration stimuli. *Behavioral Neuroscience*, 126(5), 720.
- Escanilla, O., Arrellanos, A., Karnow, A., Ennis, M., & Linster, C. (2010). Noradrenergic modulation of behavioral odor detection and discrimination thresholds in the olfactory bulb. *European Journal of Neuroscience*, 32(3), 458–468.
- Fenno, L., Yizhar, O., & Deisseroth, K. (2011). The development and application of optogenetics. *Annual Review of Neuroscience*, 34.
- Fletcher, M. L., & Chen, W. R. (2010). Neural correlates of olfactory learning: critical role of centrifugal neuromodulation. *Learning & Memory*, 17(11), 561–570.
- Foote, S., Aston-Jones, G., & Bloom, F. (1980). Impulse activity of locus coeruleus neurons in awake rats and monkeys is a function of sensory stimulation and arousal. *Proceedings of the National Academy of Sciences*, 77(5), 3033–3037.
- Foote, S. L., Freedman, R., & Oliver, A. P. (1975). Effects of putative neurotransmitters on neuronal activity in monkey auditory cortex. *Brain Research*, 86(2), 229–242.

- Grzanna, R., & Molliver, M. (1980). The locus coeruleus in the rat: an immunohistochemical delineation. *Neuroscience*, *5*(1), 21–40.
- Guerin, D., Peace, S. T., Didier, A., Linster, C., & Cleland, T. A. (2008). Noradrenergic neuromodulation in the olfactory bulb modulates odor habituation and spontaneous discrimination. *Behavioral Neuroscience*, *122*(4), 816.
- Harley, C. W., Darby-King, A., McCann, J., & McLean, J. H. (2006). β 1-adrenoceptor or α 1-adrenoceptor activation initiates early odor preference learning in rat pups: Support for the mitral cell/camp model of odor preference learning. *Learning & Memory*, *13*(1), 8–13.
- Hickey, L., Li, Y., Fyson, S. J., Watson, T. C., Perrins, R., Hewinson, J., . . . Pickering, A. E. (2014). Optoactivation of locus ceruleus neurons evokes bidirectional changes in thermal nociception in rats. *Journal of Neuroscience*, *34*(12), 4148–4160.
- Hobson, J. A., McCarley, R. W., & Wyzinski, P. W. (1975). Sleep cycle oscillation: reciprocal discharge by two brainstem neuronal groups. *Science*, *189*(4196), 55–58.
- Holets, V., Hökfelt, T., Rökaeus, Å., Terenius, L., & Goldstein, M. (1988). Locus coeruleus neurons in the rat containing neuropeptide y, tyrosine hydroxylase or galanin and their efferent projections to the spinal cord, cerebral cortex and hypothalamus. *Neuroscience*, *24*(3), 893–906.
- Jiang, M., Griff, E. R., Ennis, M., Zimmer, L. A., & Shipley, M. T. (1996). Activation of locus coeruleus enhances the responses of olfactory bulb mitral cells to weak olfactory nerve input. *Journal of Neuroscience*, *16*(19), 6319–6329.
- Kane, G. A., Vazey, E. M., Wilson, R. C., Shenhav, A., Daw, N. D., Aston-Jones,

- G., & Cohen, J. D. (2017). Increased locus coeruleus tonic activity causes disengagement from a patch-foraging task. *Cognitive, Affective, & Behavioral Neuroscience*, 17(6), 1073–1083.
- Kempadoo, K. A., Mosharov, E. V., Choi, S. J., Sulzer, D., & Kandel, E. R. (2016). Dopamine release from the locus coeruleus to the dorsal hippocampus promotes spatial learning and memory. *Proceedings of the National Academy of Sciences*, 113(51), 14835–14840.
- Kety, S. (1972). The possible role of the adrenergic systems of the cortex in learning. *Research Publications-Association for Research in Nervous and Mental Disease*, 50, 376–389.
- Lang, R., Gundlach, A. L., Holmes, F. E., Hobson, S. A., Wynick, D., Hökfelt, T., & Kofler, B. (2015). Physiology, signaling, and pharmacology of galanin peptides and receptors: three decades of emerging diversity. *Pharmacological Reviews*, 67(1), 118–175.
- Lin, J. Y. (2011). A user’s guide to channelrhodopsin variants: features, limitations and future developments. *Experimental Physiology*, 96(1), 19–25.
- Linster, C., & Devore, S. (2012). Noradrenergic and cholinergic modulation of olfactory bulb sensory processing. *Frontiers in Behavioral Neuroscience*, 6, 52.
- Linster, C., & Escanilla, O. (2018). Noradrenergic effects on olfactory perception and learning. *Brain Research*.
- Linster, C., Nai, Q., & Ennis, M. (2011). Nonlinear effects of noradrenergic modulation of olfactory bulb function in adult rodents. *Journal of Neurophysiology*, 105(4), 1432–1443.
- Loughlin, S., Foote, S., & Bloom, F. (1986). Efferent projections of nucleus locus

- coeruleus: topographic organization of cells of origin demonstrated by three-dimensional reconstruction. *Neuroscience*, 18(2), 291–306.
- Mandairon, N., Peace, S., Karnow, A., Kim, J., Ennis, M., & Linster, C. (2008). Noradrenergic modulation in the olfactory bulb influences spontaneous and reward-motivated discrimination, but not the formation of habituation memory. *European Journal of Neuroscience*, 27(5), 1210–1219.
- Manella, L. C., Alperin, S., & Linster, C. (2013). Stressors impair odor recognition memory via an olfactory bulb-dependent noradrenergic mechanism. *Frontiers in Integrative Neuroscience*, 7, 97.
- Manella, L. C., Petersen, N., & Linster, C. (2017). Stimulation of the locus ceruleus modulates signal-to-noise ratio in the olfactory bulb. *Journal of Neuroscience*, 37(48), 11605–11615.
- Mason, S. T., & Fibiger, H. C. (1979). Regional topography within noradrenergic locus coeruleus as revealed by retrograde transport of horseradish peroxidase. *Journal of Comparative Neurology*, 187(4), 703–724.
- Mason, S. T., & Iversen, S. D. (1978). Reward, attention and the dorsal noradrenergic bundle. *Brain Research*, 150(1), 135–148.
- McCall, J. G., Al-Hasani, R., Siuda, E. R., Hong, D. Y., Norris, A. J., Ford, C. P., & Bruchas, M. R. (2015). Crh engagement of the locus coeruleus noradrenergic system mediates stress-induced anxiety. *Neuron*, 87(3), 605–620.
- McLean, J. H., & Harley, C. W. (2004). Olfactory learning in the rat pup: a model that may permit visualization of a mammalian memory trace. *Neuroreport*, 15(11), 1691–1697.
- McLean, J. H., Shipley, M. T., Nickell, W. T., Aston-Jones, G., & Reyher, C. K.

- (1989). Chemoanatomical organization of the noradrenergic input from locus coeruleus to the olfactory bulb of the adult rat. *Journal of Comparative Neurology*, 285(3), 339–349.
- Mori, K. (1987). Membrane and synaptic properties of identified neurons in the olfactory bulb. *Progress in Neurobiology*, 29(3), 275–320.
- Moriceau, S., Wilson, D. A., Levine, S., & Sullivan, R. M. (2006). Dual circuitry for odor–shock conditioning during infancy: corticosterone switches between fear and attraction via amygdala. *Journal of Neuroscience*, 26(25), 6737–6748.
- Morrison, G. L., Fontaine, C. J., Harley, C. W., & Yuan, Q. (2013). A role for the anterior piriform cortex in early odor preference learning: evidence for multiple olfactory learning structures in the rat pup. *Journal of neurophysiology*, 110(1), 141–152.
- Moruzzi, G., & Magoun, H. W. (1949). Brain stem reticular formation and activation of the eeg. *Electroencephalography and Clinical Neurophysiology*, 1(1-4), 455–473.
- Nai, Q., Dong, H.-W., Hayar, A., Linster, C., & Ennis, M. (2009). Noradrenergic regulation of gabaergic inhibition of main olfactory bulb mitral cells varies as a function of concentration and receptor subtype. *Journal of Neurophysiology*, 101(5), 2472–2484.
- Nai, Q., Dong, H.-W., Linster, C., & Ennis, M. (2010). Activation of $\alpha 1$ and $\alpha 2$ noradrenergic receptors exert opposing effects on excitability of main olfactory bulb granule cells. *Neuroscience*, 169(2), 882–892.
- Neuman, R., & Harley, C. (1983). Long-lasting potentiation of the dentate gyrus population spike by norepinephrine. *Brain Research*, 273(1), 162–165.

- Pinching, A., & Powell, T. (1971). The neuron types of the glomerular layer of the olfactory bulb. *Journal of Cell Science*, 9(2), 305–345.
- Price, J., & Powell, T. (1970). The mitral and short axon cells of the olfactory bulb. *Journal of Cell Science*, 7(3), 631–651.
- Reyes, B., Drolet, G., & Van Bockstaele, E. (2008). Dynorphin and stress-related peptides in rat locus coeruleus: Contribution of amygdalar efferents. *Journal of Comparative Neurology*, 508(4), 663–675.
- Rogawski, M. A., & Aghajanian, G. K. (1982). Activation of lateral geniculate neurons by locus coeruleus or dorsal noradrenergic bundle stimulation: Selective blockade by the alpha1-adrenoceptor antagonist prazosin. *Brain Research*, 250(1), 31–39.
- Rossi, M. A., Go, V., Murphy, T., Fu, Q., Morizio, J., & Yin, H. H. (2015). A wirelessly controlled implantable led system for deep brain optogenetic stimulation. *Frontiers in Integrative Neuroscience*, 9, 8.
- Roussel, B., Buguet, A., Bobillier, P., & Jouvet, M. (1967). Locus ceruleus, paradoxical sleep, and cerebral noradrenaline. *Proceedings of Meetings of the Society of Biology and its subsidiaries*, 161(12), 2537.
- Samuels, E., & Szabadi, E. (2008). Functional neuroanatomy of the noradrenergic locus coeruleus: its roles in the regulation of arousal and autonomic function part ii: physiological and pharmacological manipulations and pathological alterations of locus coeruleus activity in humans. *Current Neuropharmacology*, 6(3), 254–285.
- Sara, S. J. (1985a). The locus coeruleus and cognitive function: attempts to relate noradrenergic enhancement of signal/noise in the brain to behavior. *Physiological*

- Psychology*, 13(3), 151–162.
- Sara, S. J. (1985b). Noradrenergic modulation of selective attention: its role in memory retrieval. *Annals of the New York Academy of Sciences*, 444(1), 178–193.
- Sara, S. J. (2009). The locus coeruleus and noradrenergic modulation of cognition. *Nature Reviews Neuroscience*, 10(3), 211.
- Schwarz, L. A., & Luo, L. (2015). Organization of the locus coeruleus-norepinephrine system. *Current Biology*, 25(21), R1051–R1056.
- Shakhawat, A. M., Gheidi, A., MacIntyre, I. T., Walsh, M. L., Harley, C. W., & Yuan, Q. (2015). Arc-expressing neuronal ensembles supporting pattern separation require adrenergic activity in anterior piriform cortex: An exploration of neural constraints on learning. *Journal of Neuroscience*, 35(41), 14070–14075.
- Shakhawat, A. M., Harley, C. W., & Yuan, Q. (2012). Olfactory bulb $\alpha 2$ -adrenoceptor activation promotes rat pup odor-preference learning via a camp-independent mechanism. *Learning & Memory*, 19(11), 499–502.
- Shiple, M. T., Fu, L., Ennis, M., Liu, W.-L., & Aston-Jones, G. (1996). Dendrites of locus coeruleus neurons extend preferentially into two pericoerulear zones. *Journal of Comparative Neurology*, 365(1), 56–68.
- Shiple, M. T., Halloran, F. J., & de la Torre, J. (1985). Surprisingly rich projection from locus coeruleus to the olfactory bulb in the rat. *Brain Research*, 329(1-2), 294–299.
- Simpson, K. L., Altman, D. W., Wang, L., Kirifides, M. L., Lin, R. C.-S., & Waterhouse, B. D. (1997). Lateralization and functional organization of the locus coeruleus projection to the trigeminal somatosensory pathway in rat. *Journal*

- of *Comparative Neurology*, 385(1), 135–147.
- Sullivan, R. M., Hofer, M. A., & Brake, S. C. (1986). Olfactory-guided orientation in neonatal rats is enhanced by a conditioned change in behavioral state. *Developmental Psychobiology: The Journal of the International Society for Developmental Psychobiology*, 19(6), 615–623.
- Sullivan, R. M., Landers, M., Yeaman, B., & Wilson, D. A. (2000). Neurophysiology: Good memories of bad events in infancy. *Nature*, 407(6800), 38.
- Sullivan, R. M., Stackenwalt, G., Nasr, F., Lemon, C., & Wilson, D. A. (2000). Association of an odor with an activation of olfactory bulb noradrenergic β -receptors or locus coeruleus stimulation is sufficient to produce learned approach responses to that odor in neonatal rats. *Behavioral Neuroscience*, 114(5), 957.
- Sullivan, R. M., & Wilson, D. A. (1991). The role of norepinephrine in the expression of learned olfactory neurobehavioral responses in infant rats. *Psychobiology*, 19(4), 308–312.
- Sullivan, R. M., Wilson, D. A., & Leon, M. (1989). Associative processes in early olfactory preference acquisition: Neural and behavioral consequences. *Psychobiology*, 17(1), 29–33.
- Swanson, L. (1976). The locus coeruleus: a cytoarchitectonic, golgi and immunohistochemical study in the albino rat. *Brain Research*, 110(1), 39–56.
- Swanson, L., & Hartman, B. (1975). The central adrenergic system. an immunofluorescence study of the location of cell bodies and their efferent connections in the rat utilizing dopamine-b-hydroxylase as a marker. *Journal of Comparative Neurology*, 163(4), 467–505.
- Tsai, H.-C., Zhang, F., Adamantidis, A., Stuber, G. D., Bonci, A., De Lecea, L., &

- Deisseroth, K. (2009). Phasic firing in dopaminergic neurons is sufficient for behavioral conditioning. *Science*, *324*(5930), 1080–1084.
- Uematsu, A., Tan, B. Z., & Johansen, J. P. (2015). Projection specificity in heterogeneous locus coeruleus cell populations: implications for learning and memory. *Learning & Memory*, *22*(9), 444–451.
- Vanderwolf, C., & Robinson, T. (1981). Reticulo-cortical activity and behavior: A critique of the arousal theory and a new synthesis. *Behavioral and Brain Sciences*, *4*(3), 459–476.
- Veyrac, A., Nguyen, V., Marien, M., Didier, A., & Jourdan, F. (2007). Noradrenergic control of odor recognition in a nonassociative olfactory learning task in the mouse. *Learning & Memory*, *14*(12), 847–854.
- Wenzel, J., & Wenzel, K. (1812). *De penitiori structura cerebri hominis et brutorum* (Vol. 2). Cotta.
- Wilson, D. A., & Sullivan, R. M. (1994). Neurobiology of associative learning in the neonate: early olfactory learning. *Behavioral and Neural Biology*, *61*(1), 1–18.
- Woo, C. C., & Leon, M. (1995). Distribution and development of β -adrenergic receptors in the rat olfactory bulb. *Journal of Comparative Neurology*, *352*(1), 1–10.
- Yuan, Q. (2009). Theta bursts in the olfactory nerve paired with β -adrenoceptor activation induce calcium elevation in mitral cells: A mechanism for odor preference learning in the neonate rat. *Learning & Memory*, *16*(11), 676–681.
- Yuan, Q., Harley, C. W., Bruce, J. C., Darby-King, A., & McLean, J. H. (2000). Isoproterenol increases creb phosphorylation and olfactory nerve-evoked potentials in normal and 5-HT-depleted olfactory bulbs in rat pups only at doses that

- produce odor preference learning. *Learning & Memory*, 7(6), 413–421.
- Yuan, Q., Harley, C. W., & McLean, J. H. (2003). Mitral cell $\beta 1$ and 5-HT_{2A} receptor colocalization and cAMP coregulation: A new model of norepinephrine-induced learning in the olfactory bulb. *Learning & Memory*, 10(1), 5–15.
- Yuan, Q., Shakhawat, A. M., & Harley, C. W. (2014). Mechanisms underlying early odor preference learning in rats. In *Progress in brain research* (Vol. 208, pp. 115–156). Elsevier.